Electronic Supplementary Material (ESI) for Organic Chemistry Frontiers.

Supporting Information

Synthesis and Characterization of Photochromic Triethylene Glycol-Containing Spiropyrans and Their Assembly in Solution

Yiwei Zhang,[a,b] Maggie Ng,[b] Michael Ho-Yeung Chan,[b] Nathan Man-Wai Wu,[b] Lixin Wu*[a] and Vivian Wing-Wah Yam*[a,b]

[a]State Key Laboratory of Supramolecular Structure and Materials and College of Chemistry, Jilin University, Changchun 130012, P. R. China

[b]Institute of Molecular Functional Materials and Department of Chemistry, The University of Hong Kong, Pokfulam Road, Hong Kong, P. R. China

Table S1. The first twenty singlet excited states (S_n) of the closed and open forms of **5** computed by TDDFT/PCM using THF as the solvent.

Compound	S_n	Excitation[a] (Coefficient)[b]	Vertical excitation wavelength / nm	f[c]
5	S_1	H–20→L (0.63)	305	0.000
Closed	S_2	H–2→L (0.68)	292	0.252
	S_3	H–2→L+1 (0.38)	278	0.010
		H→L (–0.37)		
		H–6→L (–0.33)		
	S_4	H–2→L+1 (0.44)	269	0.115
		H→L (0.39)		
	S_5	H–26→L (0.62)	267	0.000
	S_6	H→L+1 (0.49)	254	0.043
	S_7	H–6→L (0.40)	250	0.369
	S_8	H–6→L (0.31)	249	0.401
		H–3→L+2 (–0.31)		
	S_9	H→L+4 (0.44)	244	0.036
	S_{10}	H–1→L+2 (0.41)	243	0.538
	S_{11}	H–1→L (0.62)	241	0.003
		H→L (0.33)		
	S_{12}	H→L+6 (0.48)	218	0.249
	S_{13}	H–6→L+1 (0.54)	213	0.208
	S_{14}	H–1→L+3 (0.40)	213	0.046
	S_{15}	H–3→L (0.70)	212	0.000
	S_{16}	H–1→L+1 (0.60)	209	0.001
		H→L+1 (0.35)		
	S_{17}	H–4→L (0.68)	206	0.003
	S_{18}	H–17→L+3 (0.56)	205	0.011
	S_{19}	H–3→L+2 (0.35)	199	0.675
	S_{20}	H→L+3 (0.29)	195	0.141
		H→L+2 (–0.28)		
		H–1→L+7 (0.28)		
		H–1→L+3 (–0.27)		
5	S_1	H→L (0.69)	455	0.926
Open	S_2	H–4→L (0.64)	358	0.000
	S_3	H–3→L (0.58)	317	0.069
	S_4	H–1→L (0.63)	311	0.040
	S_5	H–19→L (0.59)	306	0.000
	S_6	H→L+1 (0.59)	301	0.559
	S_7	H–2→L (0.70)	272	0.001
	S_8	H–23→L+1 (0.61)	265	0.000
		H–23→L (0.32)		

S_9	H–10→L (0.59)	259	0.052
S_{10}	H–4→L+1 (0.56)	252	0.001
S_{11}	H–15→L (0.53)	251	0.036
S_{12}	H–2→L+3 (0.43)	250	0.126
S_{13}	H–3→L+1 (0.48)	246	0.052
S_{14}	H–1→L+3 (0.54)	242	0.613
S_{15}	H–1→L+1 (0.61)	232	0.010
S_{16}	H→L+2 (0.42)	231	0.067
S_{17}	H→L+4 (0.52)	226	0.021
S_{18}	H–8→L (0.55)	222	0.001
S_{19}	H–1→L+5 (0.50)	214	0.009
S_{20}	H–2→L+1 (0.65)	213	0.000

[a] Orbitals involved in the major excitation (H = HOMO and L = LUMO).

[b] The coefficients in the configuration interaction (CI) expansion that are less than 0.3 are not listed.

[c] Oscillator strengths.

Table S2. Cartesian coordinates of the ground-state geometry of the closed form of compound **5** optimized at the CAM-B3LYP level.

1	C	-8.012456	-1.186784	-2.277769	54	H	6.235481	3.158658	0.601264
2	C	-9.173074	-1.964156	-2.271038	55	H	5.536310	2.220085	1.937695
3	C	-7.998802	0.089972	-2.820034	56	C	3.601666	-1.208053	-0.261696
4	C	-10.343211	-1.471855	-2.812411	57	H	3.270751	-1.430226	-1.283816
5	C	-9.190119	0.578375	-3.365022	58	H	4.288360	-0.358107	-0.277014
6	H	-7.103539	0.702418	-2.819928	59	C	4.290673	-2.422479	0.325507
7	C	-10.350523	-0.185269	-3.363642	60	H	4.716307	-2.173889	1.308124
8	H	-11.249682	-2.070192	-2.807644	61	H	3.562723	-3.234119	0.469230
9	H	-9.203495	1.576729	-3.790760	62	O	0.628776	7.146969	0.165094
10	H	-11.264524	0.215922	-3.788347	63	C	1.186676	8.393089	0.514494
11	N	-6.959317	-1.894599	-1.679092	64	H	2.111653	8.582694	-0.049264
12	C	-8.852777	-3.315205	-1.662518	65	H	1.434624	8.427030	1.585289
13	C	-9.930728	-3.861228	-0.729549	66	C	0.160413	9.459426	0.191149
14	H	-9.588720	-4.775612	-0.234917	67	H	-0.090035	9.422716	-0.879210
15	H	-10.211123	-3.134723	0.033386	68	H	-0.763804	9.269768	0.756368
16	H	-10.824084	-4.115067	-1.306178	69	O	0.719778	10.704164	0.537834
17	C	-8.592275	-4.322556	-2.796257	70	C	-0.145120	11.787120	0.285012
18	H	-9.498412	-4.427629	-3.397406	71	H	-0.409584	11.839893	-0.781252
19	H	-7.788527	-3.986118	-3.456030	72	H	-1.079982	11.686750	0.855637
20	H	-8.332179	-5.308397	-2.401130	73	C	0.573756	13.054997	0.697976
21	C	-5.760007	-1.214907	-1.238936	74	H	0.839567	13.000900	1.764586
22	H	-5.987328	-0.196471	-0.902329	75	H	1.510087	13.153651	0.128021
23	H	-5.338747	-1.751775	-0.386259	76	O	-0.290406	14.135850	0.444852
24	C	-4.727151	-1.155848	-2.369425	77	C	0.278675	15.375568	0.793343
25	H	-4.350966	-2.152731	-2.602434	78	H	1.195956	15.574190	0.221203
26	H	-5.172323	-0.739456	-3.273716	79	H	-0.454950	16.150811	0.565687
27	N	-3.599576	-0.310424	-2.015082	80	H	0.524132	15.420782	1.863812
28	C	-2.418150	-0.647307	-1.456819	81	O	6.127569	1.119388	0.282639
29	C	-1.768422	0.553670	-1.268433	82	C	7.349300	0.741863	0.877223
30	H	-2.148873	-1.670729	-1.251062	83	H	8.055254	1.584976	0.890092
31	N	-3.694507	1.015966	-2.160944	84	H	7.196045	0.420594	1.917744
32	N	-2.593698	1.540762	-1.716071	85	C	7.934899	-0.401043	0.072487
33	C	-0.442602	0.836840	-0.705733	86	H	8.181270	-0.056968	-0.942990
34	C	-0.048267	2.163526	-0.513843	87	H	7.194935	-1.207630	-0.021264
35	C	0.425653	-0.190782	-0.352127	88	O	9.093039	-0.830845	0.752571
36	C	1.196515	2.457401	0.029225	89	C	9.791517	-1.861450	0.090186
37	H	-0.739405	2.951754	-0.778054	90	H	10.064357	-1.557694	-0.931418
38	C	1.678247	0.100929	0.175321	91	H	9.188511	-2.777546	0.021524
39	H	0.159691	-1.234253	-0.476859	92	C	11.047693	-2.137447	0.891736
40	C	2.091353	1.423010	0.359889	93	H	11.653271	-1.221286	0.958640
41	O	1.621797	3.720818	0.299547	94	H	10.777618	-2.432362	1.916801
42	O	2.475324	-0.939806	0.571304	95	O	11.760714	-3.163636	0.241584
43	O	3.308046	1.643627	0.937046	96	C	12.972497	-3.473017	0.890061
44	C	0.755965	4.805786	0.010738	97	H	13.454501	-4.271785	0.323786
45	H	0.521217	4.845158	-1.058982	98	H	13.643781	-2.603609	0.922079
46	H	-0.182295	4.713717	0.569288	99	H	12.803255	-3.817331	1.919787
47	C	1.486930	6.064725	0.430670	100	O	5.300767	-2.807622	-0.579793
48	H	2.427790	6.157345	-0.131499	101	C	6.126402	-3.839675	-0.089384
49	H	1.738769	6.010077	1.499693	102	H	6.725600	-3.488876	0.763936
50	C	4.211682	2.548713	0.294527	103	H	5.526530	-4.694697	0.252573
51	H	4.202351	2.386014	-0.789271	104	C	7.052530	-4.251424	-1.217147
52	H	3.917078	3.580234	0.495213	105	H	7.440446	-3.349702	-1.713574
53	C	5.592840	2.298692	0.842427	106	H	6.508054	-4.838125	-1.970554

107	O	8.101952	-5.003522	-0.653365
108	C	8.983615	-5.533689	-1.619098
109	H	9.357371	-4.742001	-2.284119
110	H	8.475442	-6.283844	-2.242330
111	C	10.141339	-6.173533	-0.880939
112	H	10.699604	-5.402453	-0.331354
113	H	9.754610	-6.902763	-0.152299
114	O	10.957035	-6.804746	-1.841617
115	C	12.087867	-7.415582	-1.269802
116	H	12.659397	-7.875936	-2.077829
117	H	12.726816	-6.684180	-0.754490
118	H	11.805369	-8.193596	-0.546073
119	C	-7.516683	-2.977658	-0.901433
120	C	-6.559405	-4.121377	-0.749977
121	C	-7.611870	-2.993254	1.573024
122	C	-6.251547	-4.667628	0.425997
123	H	-6.128695	-4.497095	-1.670099
124	C	-6.810020	-4.142847	1.663455
125	C	-8.145101	-2.398156	2.718470
126	H	-5.564345	-5.505790	0.484885
127	C	-6.561702	-4.694410	2.912562
128	C	-7.897014	-2.954796	3.958683
129	H	-8.752639	-1.507381	2.612754
130	C	-7.109655	-4.100305	4.040687
131	H	-5.944249	-5.577994	3.015399
132	H	-8.304272	-2.519349	4.861448
133	O	-7.881784	-2.406510	0.395281
134	N	-6.849116	-4.687521	5.343081
135	O	-7.340536	-4.150041	6.328469
136	O	-6.150415	-5.693160	5.395013

Table S3. Cartesian coordinates of the ground-state geometry of the open form of compound **5** optimized at the CAM-B3LYP level.

1	C	4.016991	-8.110432	0.218471	54	H	-4.748391	4.253175	-0.444968
2	C	5.401768	-8.154177	0.124671	55	H	-4.322979	3.746900	1.205307
3	C	3.228300	-9.248524	0.203166	56	C	-0.148065	2.513192	-0.070726
4	C	6.045137	-9.374028	0.018928	57	H	-0.324729	2.317860	-1.135231
5	C	3.887015	-10.472558	0.095813	58	H	-0.942535	3.160844	0.301094
6	H	2.147282	-9.207472	0.266165	59	C	1.205286	3.167700	0.122536
7	C	5.275170	-10.538058	0.006116	60	H	1.419023	3.258606	1.197780
8	H	7.126492	-9.431502	-0.054481	61	H	1.995756	2.545872	-0.323463
9	H	3.303408	-11.386541	0.080455	62	C	4.668799	-5.921106	0.276405
10	H	5.762644	-11.503199	-0.076963	63	C	4.501220	-4.533456	0.324299
11	N	3.615660	-6.756507	0.322559	64	H	3.503291	-4.128296	0.388385
12	C	5.953527	-6.744467	0.158855	65	C	5.523644	-3.603580	0.305256
13	C	6.855988	-6.553007	1.393361	66	H	6.549166	-3.957085	0.260243
14	H	7.255918	-5.539999	1.452128	67	C	5.390316	-2.197244	0.347956
15	H	6.308907	-6.761400	2.315352	68	C	6.577718	-1.435679	0.360828
16	H	7.698410	-7.245779	1.332840	69	C	4.094595	-1.507363	0.386345
17	C	6.708933	-6.435199	-1.147344	70	C	6.542240	-0.067505	0.425169
18	H	7.547991	-7.127198	-1.249125	71	H	7.539920	-1.933653	0.323500
19	H	6.058514	-6.559441	-2.015961	72	C	4.139966	-0.058993	0.470084
20	H	7.106436	-5.419669	-1.157352	73	C	5.305862	0.632810	0.486412
21	C	2.227078	-6.337468	0.437013	74	H	3.182547	0.448640	0.520640
22	H	1.661754	-7.142381	0.905895	75	H	5.322649	1.713930	0.545608
23	H	2.177058	-5.481043	1.110093	76	N	7.774516	0.672112	0.436686
24	C	1.627833	-5.968185	-0.932282	77	O	7.714802	1.898831	0.496503
25	H	2.382599	-5.476810	-1.548946	78	O	8.836501	0.053317	0.385896
26	H	1.269806	-6.850310	-1.462479	79	O	2.997826	-2.106028	0.350423
27	N	0.506805	-5.063000	-0.784809	80	O	-7.781706	-1.819739	-0.113944
28	C	0.551926	-3.736432	-0.544009	81	C	-9.124023	-1.405190	-0.004089
29	C	-0.768074	-3.368203	-0.421591	82	H	-9.357304	-0.625430	-0.743658
30	H	1.476516	-3.180255	-0.468536	83	H	-9.328223	-0.991291	0.994025
31	N	-0.759200	-5.506985	-0.808508	84	C	-9.997775	-2.618821	-0.246092
32	N	-1.531068	-4.485006	-0.595011	85	H	-9.788990	-3.034368	-1.242822
33	C	-1.323896	-2.036483	-0.156235	86	H	-9.766666	-3.397986	0.494954
34	C	-2.707008	-1.837716	-0.171942	87	O	-11.338755	-2.202515	-0.141983
35	C	-0.473678	-0.968405	0.108897	88	C	-12.259132	-3.248072	-0.352214
36	C	-3.227240	-0.576269	0.085586	89	H	-12.135317	-3.687086	-1.353055
37	H	-3.354346	-2.680840	-0.370124	90	H	-12.117342	-4.052531	0.384292
38	C	-0.993032	0.302364	0.342580	91	C	-13.651879	-2.667851	-0.216023
39	H	0.603466	-1.095596	0.150738	92	H	-13.775201	-2.228409	0.785450
40	C	-2.374748	0.516755	0.332512	93	H	-13.791470	-1.860709	-0.951106
41	O	-4.559505	-0.305148	0.146010	94	O	-14.570579	-3.711854	-0.428424
42	O	-0.095171	1.283457	0.653383	95	C	-15.907922	-3.284413	-0.323844
43	O	-2.870479	1.750087	0.661099	96	H	-16.144205	-2.510704	-1.067990
44	C	-5.476421	-1.365905	-0.061262	97	H	-16.546129	-4.151852	-0.500765
45	H	-5.357807	-1.796362	-1.062219	98	H	-16.125793	-2.879639	0.674593
46	H	-5.325697	-2.160563	0.678112	99	O	-2.785393	4.599791	0.106908
47	C	-6.863018	-0.773926	0.088624	100	C	-2.932728	5.868571	0.700536
48	H	-7.008992	0.029444	-0.648444	101	H	-3.791291	6.406722	0.272652
49	H	-6.975171	-0.334168	1.090181	102	H	-3.100217	5.780561	1.783828
50	C	-3.647534	2.424491	-0.333607	103	C	-1.658511	6.645544	0.439178
51	H	-3.083745	2.484987	-1.271949	104	H	-1.521757	6.784287	-0.643555
52	H	-4.578747	1.883245	-0.513609	105	H	-0.791516	6.079384	0.808118
53	C	-3.952063	3.810932	0.172203	106	O	-1.779273	7.886552	1.095818

107	C	-0.650050	8.710365	0.929557
108	H	-0.470941	8.925738	-0.134584
109	H	0.253924	8.226763	1.328857
110	C	-0.907432	10.004270	1.674195
111	H	-1.813754	10.486915	1.278085
112	H	-1.083952	9.791500	2.739423
113	O	0.221818	10.825077	1.500688
114	C	0.095173	12.064771	2.155805
115	H	1.008550	12.631717	1.967931
116	H	-0.763389	12.636546	1.776101
117	H	-0.028471	11.937729	3.240597
118	O	1.162026	4.434951	-0.492638
119	C	2.392424	5.118455	-0.424867
120	H	2.678921	5.313906	0.618735
121	H	3.196504	4.526351	-0.885991
122	C	2.234380	6.428941	-1.168220
123	H	1.431904	7.024353	-0.709292
124	H	1.948049	6.233142	-2.212078
125	O	3.466292	7.106765	-1.098777
126	C	3.440600	8.364809	-1.732190
127	H	2.689197	9.022821	-1.271288
128	H	3.188139	8.264934	-2.798119
129	C	4.818022	8.978554	-1.587910
130	H	5.068612	9.082405	-0.521397
131	H	5.569506	8.314642	-2.041506
132	O	4.795652	10.231273	-2.228056
133	C	6.032543	10.899087	-2.150643
134	H	5.925086	11.853469	-2.669075
135	H	6.323660	11.090822	-1.108215
136	H	6.834663	10.321118	-2.631084

Table S4. Cartesian coordinates of the dimer of the open form of compound **5** optimized at the PBE0-D3(BJ) level.

1	C	6.786623	-8.206997	-0.655187	54	H	-4.468351	1.541406	0.163176
2	C	8.146537	-7.947924	-0.817025	55	H	-4.307368	1.206694	1.902243
3	C	6.223468	-9.444745	-0.933691	56	C	0.330144	0.555892	0.652592
4	C	8.994107	-8.956890	-1.240160	57	H	0.826442	0.062236	-0.193802
5	C	7.088119	-10.452996	-1.363791	58	H	-0.646011	0.934054	0.331417
6	H	5.158260	-9.628085	-0.837894	59	C	1.186870	1.686434	1.164396
7	C	8.454707	-10.218332	-1.510508	60	H	0.705927	2.158136	2.034243
8	H	10.057700	-8.774099	-1.365788	61	H	2.155269	1.287972	1.502094
9	H	6.682795	-11.433703	-1.593759	62	C	7.025847	-5.997720	-0.122846
10	H	9.104359	-11.020049	-1.847764	63	C	6.588746	-4.713011	0.169390
11	N	6.159337	-7.038146	-0.194066	64	H	5.528552	-4.526349	0.288509
12	C	8.426654	-6.504625	-0.459020	65	C	7.403349	-3.591207	0.281556
13	C	9.340229	-6.434935	0.776971	66	H	8.482650	-3.718808	0.245998
14	H	8.929160	-7.029904	1.597972	67	C	6.968115	-2.267420	0.455876
15	H	10.321908	-6.846962	0.524475	68	C	7.966492	-1.274119	0.596846
16	H	9.476163	-5.412535	1.135709	69	C	5.543810	-1.875409	0.487966
17	C	9.040516	-5.764832	-1.655674	70	C	7.633048	0.041062	0.782288
18	H	9.966642	-6.264478	-1.954463	71	H	9.015326	-1.552299	0.574408
19	H	8.360921	-5.767192	-2.512123	72	C	5.282290	-0.464585	0.707434
20	H	9.281848	-4.728226	-1.411595	73	C	6.273363	0.456081	0.854759
21	C	4.754716	-6.950250	0.137044	74	H	4.236964	-0.173006	0.748883
22	H	4.409931	-7.937612	0.450658	75	H	6.055130	1.504509	1.039792
23	H	4.642752	-6.279260	0.992207	76	N	8.682377	1.016353	0.919262
24	C	3.912476	-6.437759	-1.034134	77	O	8.358996	2.177907	1.148076
25	H	4.405278	-5.589119	-1.513321	78	O	9.844497	0.644753	0.795841
26	H	3.752993	-7.216838	-1.782075	79	O	4.609374	-2.685688	0.334571
27	N	2.625301	-5.993795	-0.559608	80	O	-6.363826	-5.181104	0.224472
28	C	2.267975	-4.750317	-0.179664	81	C	-7.663163	-4.911829	-0.244142
29	C	0.953551	-4.889171	0.226642	82	H	-7.637740	-4.543275	-1.282433
30	H	2.947790	-3.908452	-0.220596	83	H	-8.161581	-4.140780	0.361705
31	N	1.620734	-6.865530	-0.388615	84	C	-8.456159	-6.197651	-0.174108
32	N	0.606721	-6.199313	0.080025	85	H	-7.959732	-6.978046	-0.773013
33	C	0.031961	-3.842663	0.665765	86	H	-8.493672	-6.553760	0.867804
34	C	-1.351922	-4.062496	0.654263	87	O	-9.744293	-5.924382	-0.664583
35	C	0.537339	-2.601303	1.047136	88	C	-10.573254	-7.060389	-0.681527
36	C	-2.215658	-3.023388	0.981936	89	H	-10.156074	-7.844184	-1.334009
37	H	-1.727997	-5.046366	0.399557	90	H	-10.678678	-7.489613	0.327420
38	C	-0.332455	-1.564436	1.367592	91	C	-11.926169	-6.624389	-1.198520
39	H	1.606086	-2.415599	1.100351	92	H	-12.352251	-5.861945	-0.529034
40	C	-1.713305	-1.752102	1.318355	93	H	-11.803115	-6.161656	-2.192771
41	O	-3.567669	-3.114739	0.997127	94	O	-12.748309	-7.761093	-1.272254
42	O	0.183047	-0.354601	1.737427	95	C	-14.061630	-7.428966	-1.629172
43	O	-2.545177	-0.724887	1.649983	96	H	-14.106340	-6.904387	-2.597521
44	C	-4.187964	-4.341301	0.653842	97	H	-14.628945	-8.360189	-1.711805
45	H	-3.809348	-4.720776	-0.303365	98	H	-14.543062	-6.789799	-0.872074
46	H	-4.006469	-5.097640	1.428156	99	O	-2.631197	2.014217	0.999393
47	C	-5.660523	-4.006336	0.529388	100	C	-2.927305	3.387057	1.074182
48	H	-5.780459	-3.254003	-0.266951	101	H	-3.391854	3.742871	0.140202
49	H	-6.025434	-3.561243	1.468833	102	H	-3.630779	3.599881	1.894701
50	C	-3.350427	-0.212126	0.594970	103	C	-1.617512	4.110894	1.304068
51	H	-2.781521	-0.205442	-0.343852	104	H	-0.888039	3.787794	0.544847
52	H	-4.240552	-0.836520	0.453406	105	H	-1.216125	3.830624	2.288823
53	C	-3.768475	1.193205	0.940830	106	O	-1.859460	5.495107	1.213858

107	C	-0.690829	6.250521	1.434008	160	C	0.987077	-8.070113	2.962563
108	H	0.162557	5.823535	0.888661	161	H	1.777579	-7.718514	2.294862
109	H	-0.424904	6.279481	2.500636	162	H	0.413220	-8.835977	2.438848
110	C	-0.917631	7.653137	0.911822	163	N	0.097900	-6.971659	3.238081
111	H	-1.272071	7.599060	-0.130557	164	C	0.443156	-5.731717	3.640478
112	H	-1.692411	8.171434	1.500077	165	C	-0.762085	-5.107411	3.879159
113	O	0.315909	8.324127	0.987612	166	H	1.467055	-5.387033	3.696107
114	C	0.265274	9.622012	0.453952	167	N	-1.232854	-7.128287	3.224902
115	H	1.287209	10.006506	0.429453	168	N	-1.756504	-6.000312	3.601338
116	H	-0.123691	9.621512	-0.575755	169	C	-0.999329	-3.731583	4.302377
117	H	-0.365920	10.289185	1.061442	170	C	-2.300415	-3.226732	4.307232
118	O	1.361774	2.611329	0.118763	171	C	0.063354	-2.908462	4.663262
119	C	2.183899	3.673243	0.530773	172	C	-2.532590	-1.895939	4.634523
120	H	1.780570	4.140249	1.442691	173	H	-3.110469	-3.890587	4.036806
121	H	3.201025	3.324007	0.763525	174	C	-0.165596	-1.577279	5.004911
122	C	2.231756	4.728434	-0.550144	175	H	1.088982	-3.264853	4.662931
123	H	1.206744	4.999809	-0.850169	176	C	-1.464414	-1.046315	4.983797
124	H	2.750504	4.357303	-1.448403	177	O	-3.776886	-1.348546	4.655739
125	O	2.903071	5.826074	0.013640	178	O	0.915792	-0.868403	5.417856
126	C	2.853271	6.983261	-0.784924	179	O	-1.658626	0.247810	5.366673
127	H	1.814810	7.323879	-0.907230	180	C	-4.811029	-2.148457	4.119748
128	H	3.273606	6.791138	-1.785230	181	H	-4.502874	-2.572464	3.158361
129	C	3.661195	8.053791	-0.086232	182	H	-5.061239	-2.970509	4.804220
130	H	3.280350	8.203119	0.935365	183	C	-6.037305	-1.291033	3.904139
131	H	4.711343	7.732852	-0.006062	184	H	-5.857451	-0.581386	3.083529
132	O	3.542916	9.231718	-0.854434	185	H	-6.283796	-0.710018	4.805510
133	C	4.385687	10.248226	-0.388292	186	C	-2.296858	1.101355	4.413396
134	H	4.240626	11.121148	-1.031422	187	H	-1.879237	0.939750	3.413787
135	H	4.155352	10.535185	0.649658	188	H	-3.367453	0.877175	4.377494
136	H	5.446231	9.952438	-0.427976	189	C	-2.110793	2.528643	4.847205
137	C	2.865867	-10.744960	4.066292	190	H	-2.839011	3.156601	4.306353
138	C	4.197662	-11.128616	3.919948	191	H	-2.330663	2.621221	5.922767
139	C	1.830957	-11.663819	4.169958	192	C	1.129597	0.439853	4.896534
140	C	4.529620	-12.471608	3.880876	193	H	0.494671	0.626826	4.030342
141	C	2.178366	-13.014842	4.130350	194	H	0.905558	1.192001	5.657443
142	H	0.794414	-11.359790	4.272387	195	C	2.589358	0.493671	4.495090
143	C	3.506229	-13.417346	3.990107	196	H	3.216782	0.100291	5.311519
144	H	5.563218	-12.788107	3.770311	197	H	2.744974	-0.148030	3.612722
145	H	1.395668	-13.763252	4.208803	198	C	4.025615	-8.782043	3.949726
146	H	3.746514	-14.475706	3.963818	199	C	4.197165	-7.399347	3.936461
147	N	2.803471	-9.340686	4.091078	200	H	3.329478	-6.762390	4.049847
148	C	5.064675	-9.893695	3.827804	201	C	5.408528	-6.732395	3.805448
149	C	6.070025	-9.853237	4.989100	202	H	6.319357	-7.314641	3.682075
150	H	6.699754	-8.961418	4.950062	203	C	5.599349	-5.337434	3.812017
151	H	5.557923	-9.869214	5.954621	204	C	6.918607	-4.859850	3.643053
152	H	6.720927	-10.730780	4.933386	205	C	4.499924	-4.367599	3.983855
153	C	5.772362	-9.849668	2.466390	206	C	7.192469	-3.517103	3.665278
154	H	5.045967	-9.899265	1.651842	207	H	7.735046	-5.560443	3.498542
155	H	6.368884	-8.942550	2.346084	208	C	4.875540	-2.966845	4.009138
156	H	6.441334	-10.709351	2.367991	209	C	6.161351	-2.555165	3.862966
157	C	1.576989	-8.592997	4.281525	210	H	4.067932	-2.254559	4.144807
158	H	0.857784	-9.232244	4.796138	211	H	6.426216	-1.503946	3.878368
159	H	1.788537	-7.752528	4.947231	212	N	8.539444	-3.072241	3.455993

213	O	8.782800	-1.880397	3.602432	266	H	7.031988	4.201132	0.433744
214	O	9.389261	-3.904448	3.134134	267	H	5.437979	4.652861	-0.226417
215	O	3.310124	-4.712221	4.110428	268	O	6.664559	6.239504	0.296411
216	O	-7.071902	-2.193433	3.583119	269	C	7.212314	6.401073	-0.983328
217	C	-8.042783	-1.682540	2.706358	270	H	7.543964	7.439390	-1.072670
218	H	-7.614396	-1.493543	1.708223	271	H	8.077683	5.739166	-1.144095
219	H	-8.461671	-0.733414	3.073982	272	H	6.474583	6.198536	-1.776443
220	C	-9.127433	-2.734754	2.588323					
221	H	-8.655007	-3.729388	2.538093					
222	H	-9.774641	-2.724002	3.479020					
223	O	-9.863763	-2.461326	1.423814					
224	C	-11.005455	-3.275706	1.297883					
225	H	-10.736657	-4.341923	1.331727					
226	H	-11.722059	-3.076033	2.110487					
227	C	-11.645767	-2.949854	-0.033448					
228	H	-11.749753	-1.856456	-0.128374					
229	H	-11.000916	-3.300898	-0.853829					
230	O	-12.903410	-3.577845	-0.073418					
231	C	-13.564768	-3.351915	-1.289651					
232	H	-12.994523	-3.738260	-2.148303					
233	H	-14.526656	-3.869261	-1.245568					
234	H	-13.750451	-2.279389	-1.457796					
235	O	-0.800939	2.959228	4.565976					
236	C	-0.588711	4.303416	4.913759					
237	H	-1.326878	4.957749	4.419884					
238	H	-0.688492	4.455891	5.999895					
239	C	0.797191	4.679728	4.436399					
240	H	0.913474	4.331743	3.398597					
241	H	1.572165	4.177463	5.033440					
242	O	0.911183	6.078755	4.509959					
243	C	2.119068	6.547038	3.959847					
244	H	2.239483	6.200340	2.921637					
245	H	2.983772	6.187044	4.539521					
246	C	2.077859	8.058266	3.990034					
247	H	1.270316	8.420678	3.336525					
248	H	1.870521	8.397334	5.018586					
249	O	3.328864	8.525397	3.548894					
250	C	3.405157	9.923363	3.577498					
251	H	4.396796	10.208818	3.216148					
252	H	2.641442	10.392725	2.937076					
253	H	3.279041	10.318386	4.598639					
254	O	2.921481	1.831285	4.207227					
255	C	4.137889	1.942330	3.513709					
256	H	4.958471	1.451361	4.060832					
257	H	4.066848	1.452935	2.530896					
258	C	4.423798	3.415234	3.298795					
259	H	4.925830	3.856018	4.173657					
260	H	3.467094	3.939791	3.162715					
261	O	5.222632	3.538088	2.147337					
262	C	5.610111	4.872270	1.900297					
263	H	6.351188	5.206079	2.642678					
264	H	4.743843	5.546796	1.950963					
265	C	6.207524	4.926109	0.512534					

Table S5. Rate constant of compounds **1**–**6** in THF solution at different temperatures.

$k \times 10^2$ / s^{-1} in THF						
Compound	T / K					
	288	293	298	303	308	313
1	1.2	2.2	4.3	8.1	15.0	23.1
2	1.0	2.0	3.9	7.1	12.3	20.9
3	1.9	3.5	6.0	10.1	18.3	29.7
4	1.5	3.0	5.7	10.2	19.1	32.4
5	1.3	2.7	5.0	8.7	15.4	27.7
6	3.5	6.2	10.8	19.0	32.3	57.5

Table S6. Activation parameters of the bleaching reaction of compounds **1**–**6** in THF solution.

Compound	$\Delta H^{\neq}$ (kJ mol^{-1})	$\Delta S^{\neq}$ (J mol^{-1} K^{-1})	$\Delta G^{\neq}_{298\ K}$ (kJ mol^{-1})	E_a (kJ mol^{-1})
1	87.04 ± 0.78	23.77 ± 2.62	79.96 ± 1.56	89.54 ± 0.78
2	87.99 ± 0.56	23.08 ± 1.80	81.11 ± 1.09	90.48 ± 0.55
3	79.99 ± 0.18	0.14 ± 0.58	79.94 ± 0.35	82.48 ± 0.16
4	89.56 ± 0.43	31.60 ± 1.47	81.14 ± 0.87	92.06 ± 0.44
5	87.46 ± 0.72	23.42 ± 2.34	80.48 ± 1.42	89.96 ± 0.74
6	80.73 ± 0.43	7.66 ± 1.45	78.45 ± 0.86	83.22 ± 0.43

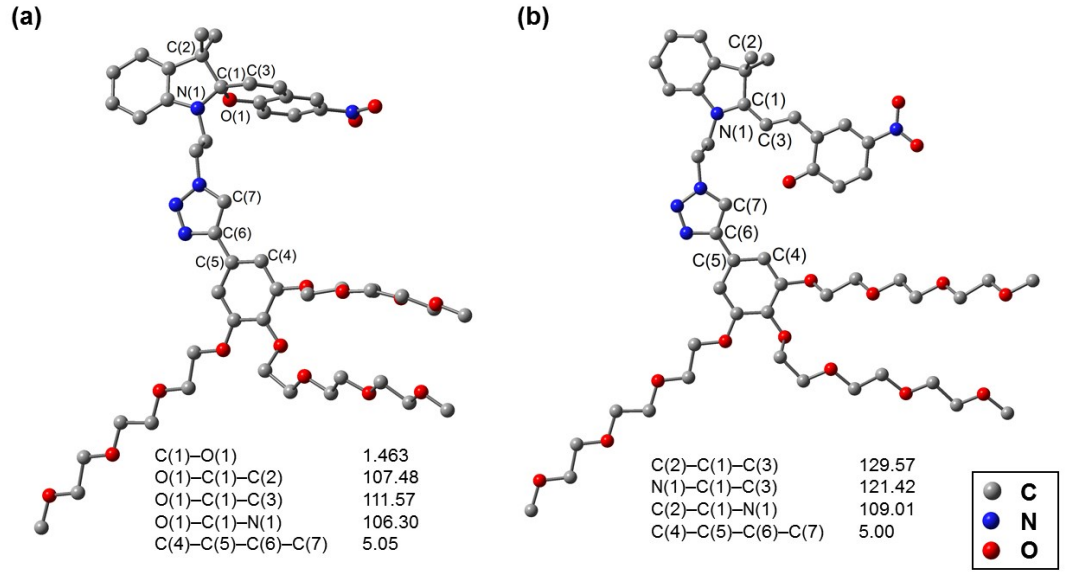

Figure S1. Ground-state geometries of (a) the closed form and (b) the open form of compound **5** optimized at the CAM-B3LYP /6-31G(d,p) level, with selected structural parameters. The bond lengths and bond angles are in Angstroms and degrees, respectively. All hydrogen atoms are omitted for clarity.

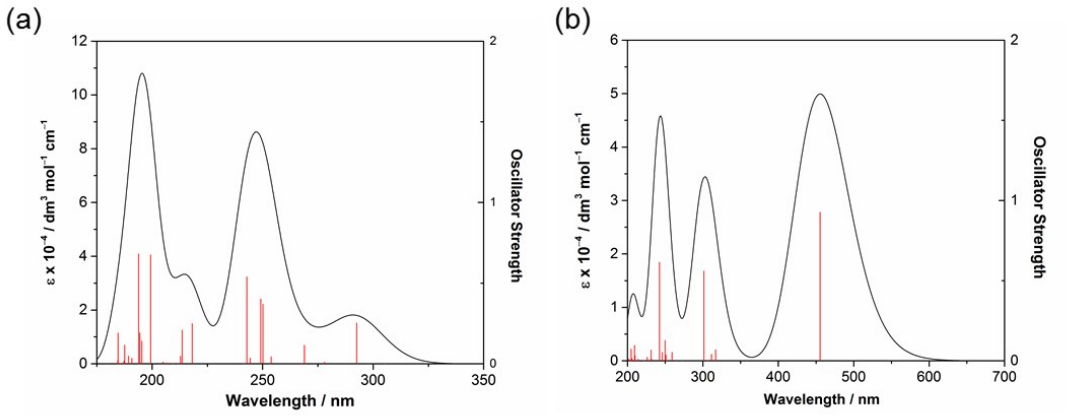

Figure S2. Simulated UV-vis spectra of (a) the closed form and (b) the open form of compound **5** computed by TDDFT/PCM in THF.

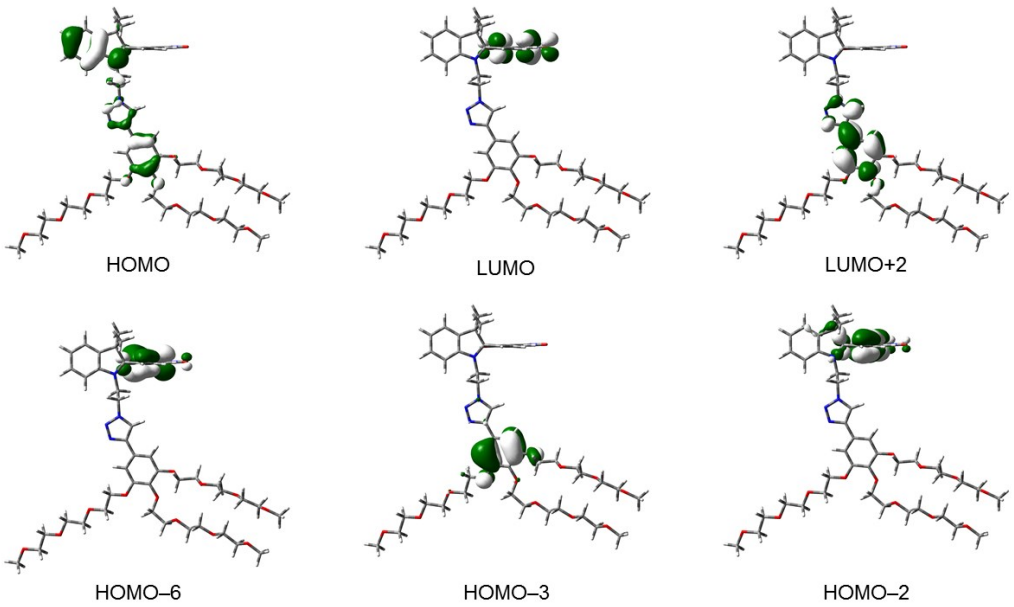

Figure S3. Spatial plots (isovalue = 0.03) of selected molecular orbitals of the closed form of **5** at the ground-state geometry optimized at the CAM-B3LYP level.

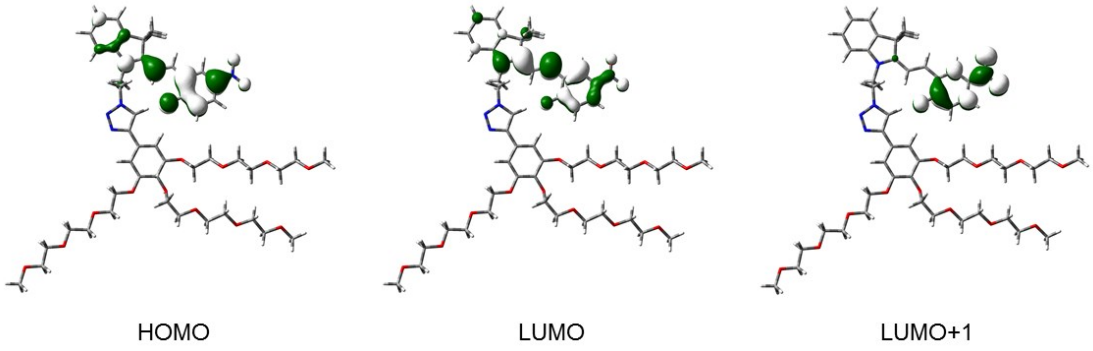

Figure S4. Spatial plots (isovalue = 0.03) of selected molecular orbitals of the open form of **5** at the ground-state geometry optimized at the CAM-B3LYP level.

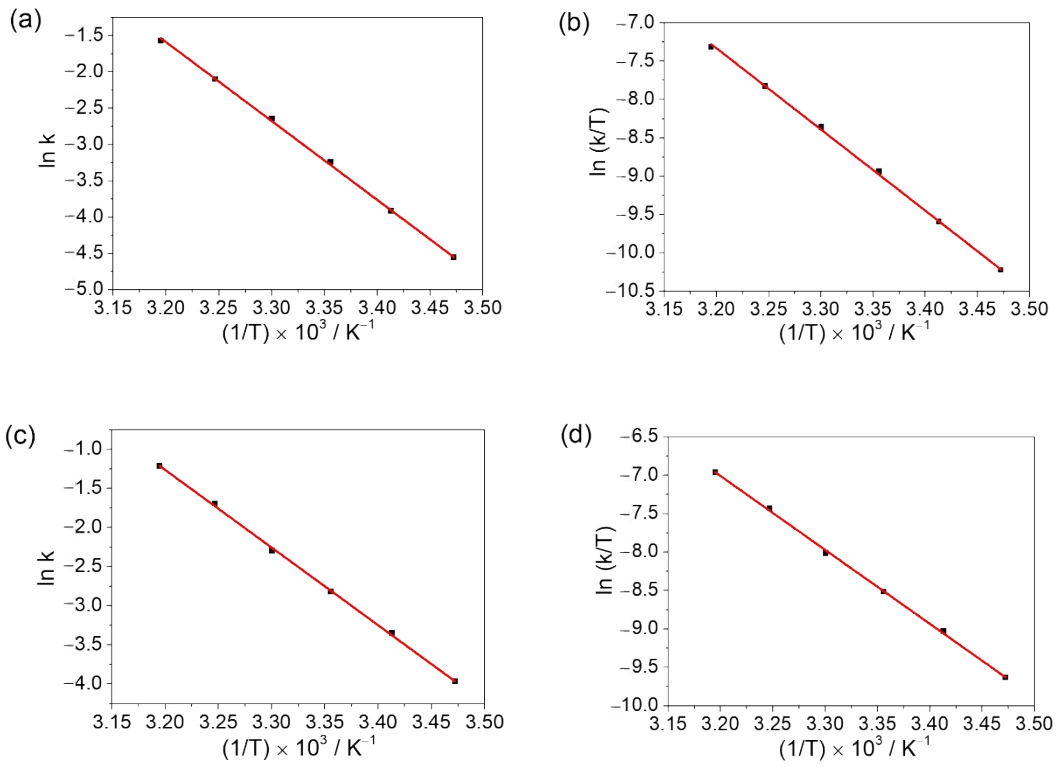

Figure S5. (a) Arrhenius and (b) Eyring plots for the thermal bleaching reaction of compound **2**; (c) Arrhenius and (d) Eyring plots for the thermal bleaching reaction of compound **3** in THF solution (conc = 4×10^{-5} M).

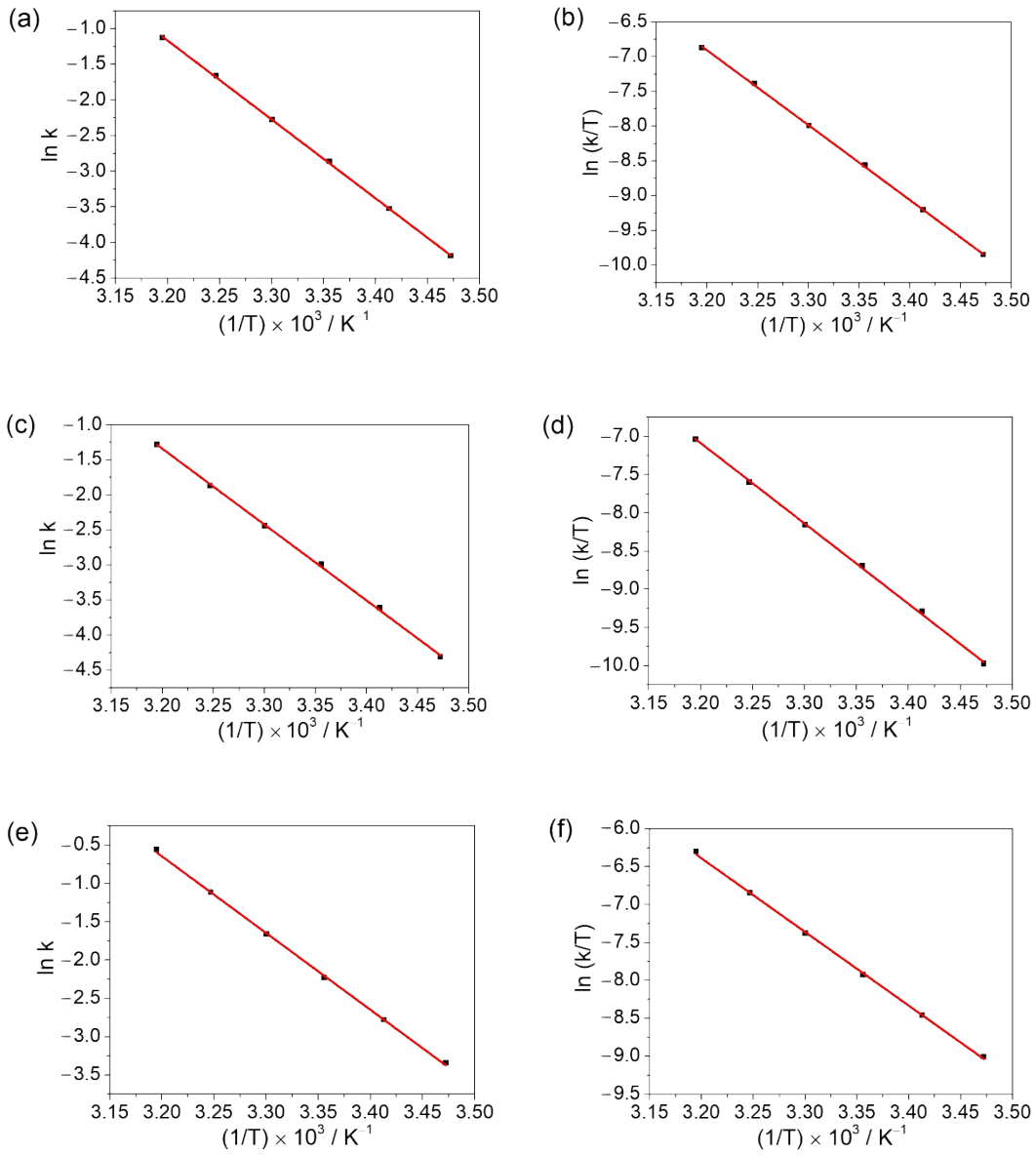

Figure S6. (a) Arrhenius and (b) Eyring plots for the thermal bleaching reaction of compound **4**; (c) Arrhenius and (d) Eyring plots for the thermal bleaching reaction of compound **5**; (e) Arrhenius and (f) Eyring plots for the thermal bleaching reaction of compound **6** in THF solution (conc = 4×10^{-5} M).

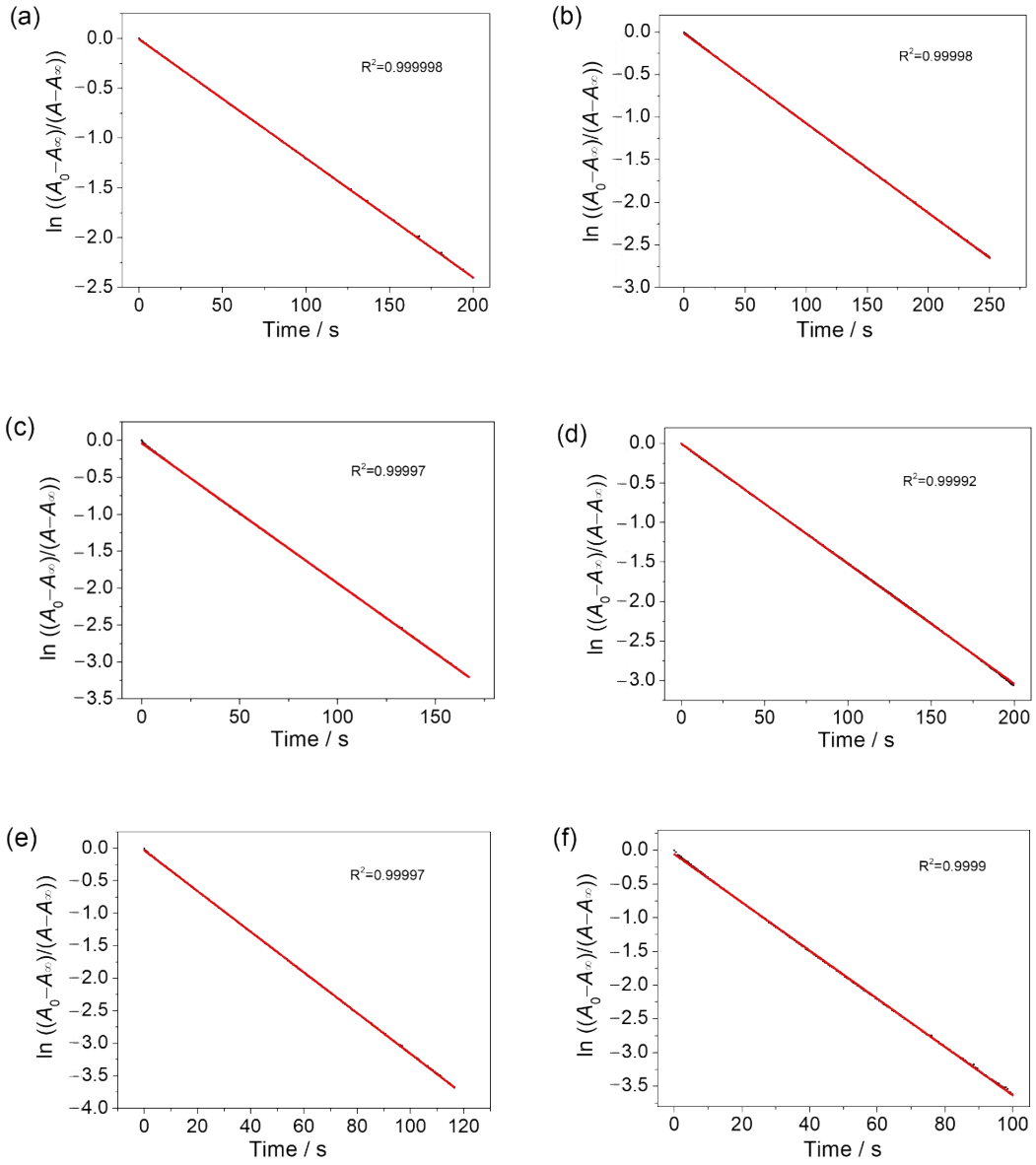

Figure S7. Plots of ln $[(A - A_\infty)/(A_0 - A_\infty)]$ against t from the bleaching reaction of compounds **1**–**6** (a–f) in THF solution at 288 K (conc = 4×10^{-5} M).

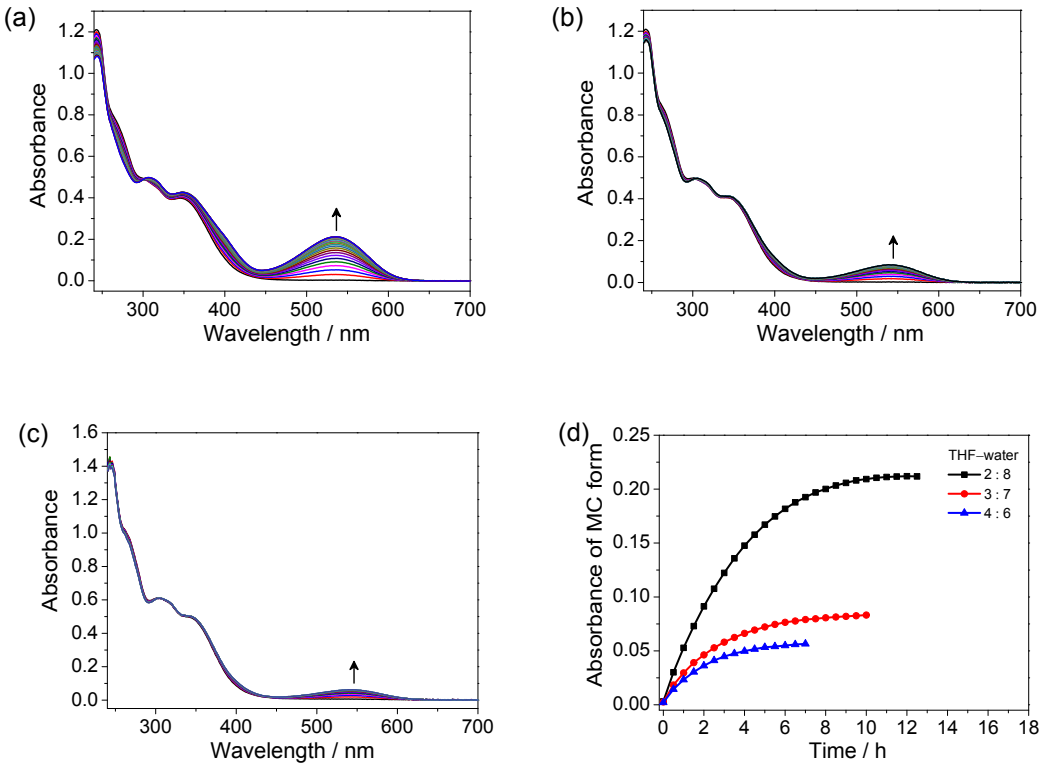

Figure S8. Time-dependent UV–vis absorption spectral changes of the closed form of compound **1** in (a) THF–water (2 : 8 v/v), (b) THF–water (3 : 7 v/v) and (c) THF–water (4 : 6 v/v) solutions in the dark. The arrows indicate the spectral changes with time. The time intervals between every two spectra were 0.5 hour; (d) absorbance traces of compound **1** in THF–water mixed solutions at the absorption maximum with time at 293 K ([**1**] = 4×10^{-5} M).

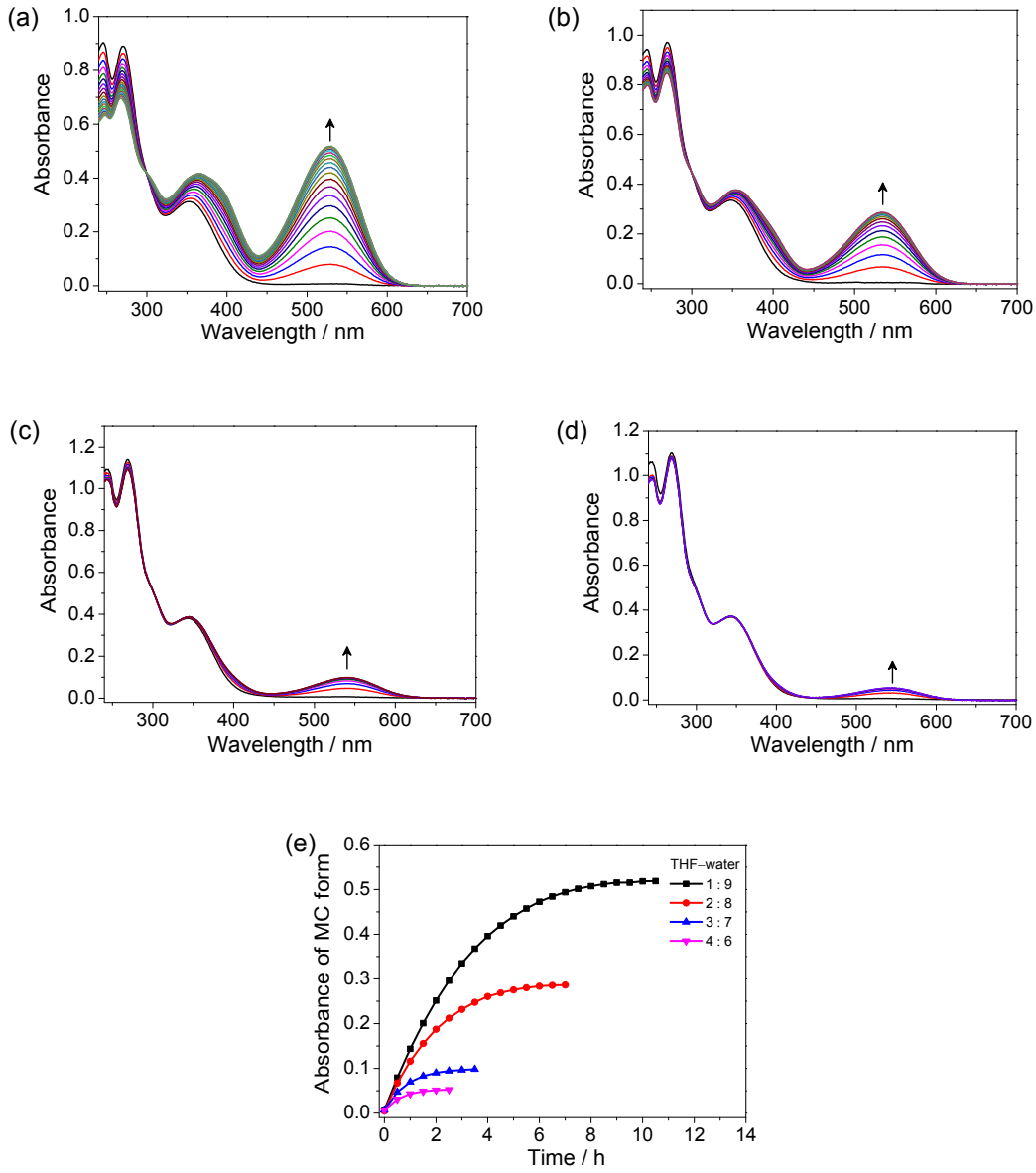

Figure S9. Time-dependent UV–vis absorption spectral changes of the closed form of compound **2** in (a) THF–water (1 : 9 v/v), (b) THF–water (2 : 8 v/v), (c) THF–water (3 : 7 v/v) and (d) THF–water (4 : 6 v/v) solutions in the dark. The arrows indicate the spectral changes with time. The time intervals between every two spectra were 0.5 hour; (e) absorbance traces of compound **2** in THF–water mixed solutions at the absorption maximum with time at 293 K ([**2**] = 4×10^{-5} M).

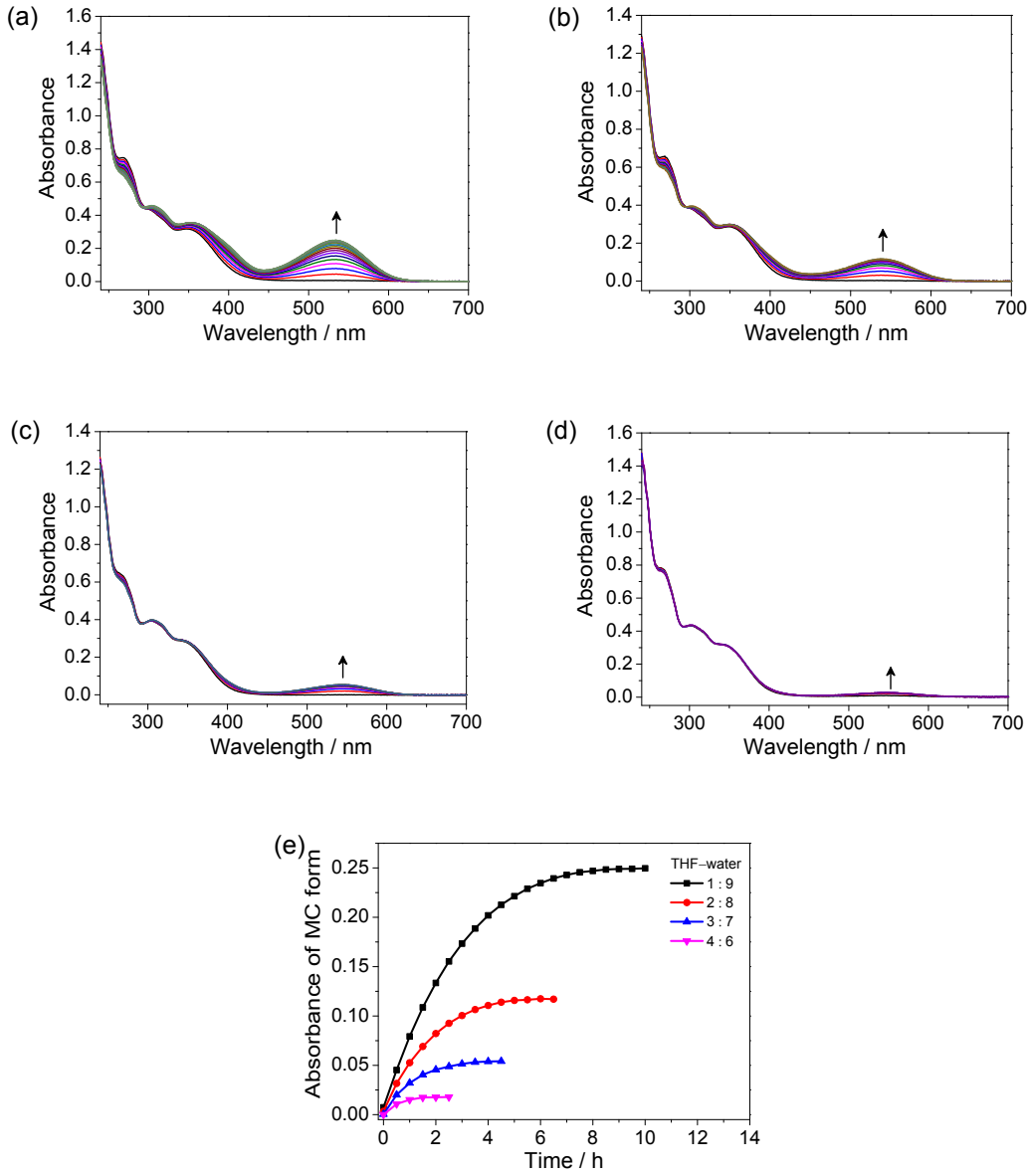

Figure S10. Time-dependent UV–vis absorption spectral changes of the closed form of compound **3** in (a) THF–water (1 : 9 v/v), (b) THF–water (2 : 8 v/v), (c) THF–water (3 : 7 v/v) and (d) THF–water (4 : 6 v/v) solutions in the dark. The arrows indicate the spectral changes with time. The time intervals between every two spectra were 0.5 hour; (e) absorbance traces of compound **3** in THF–water mixed solutions at the absorption maximum with time at 293 K ([**3**] = 4×10^{-5} M).

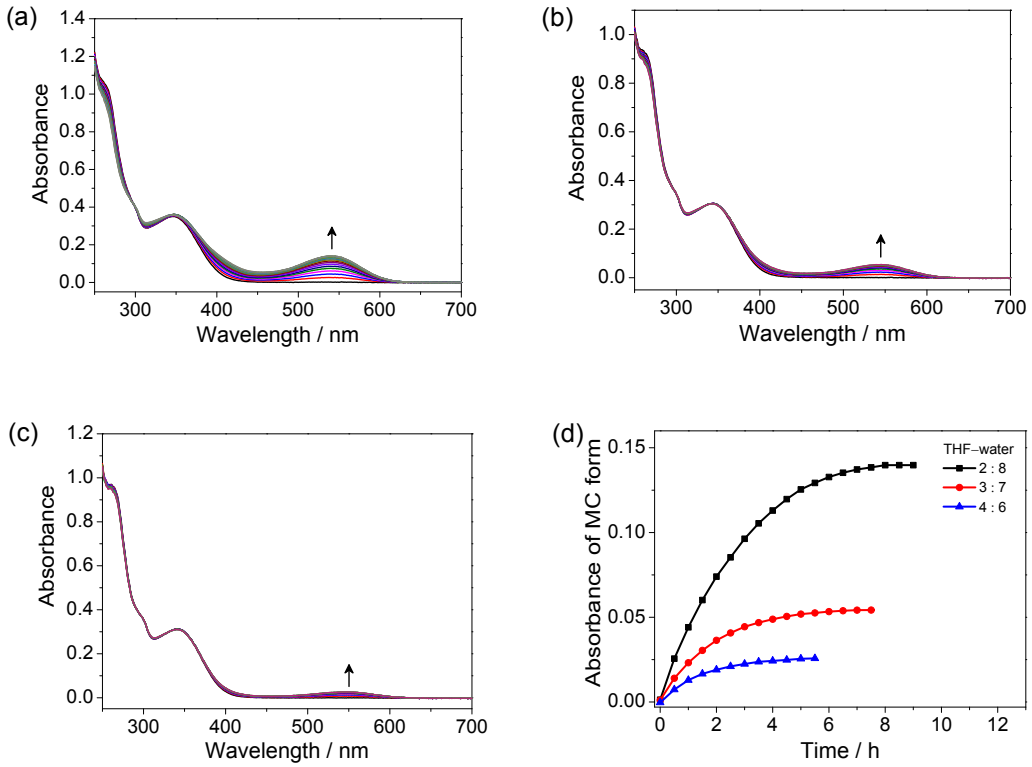

Figure S11. Time-dependent UV–vis absorption spectral changes of the closed form of compound **4** in (a) THF–water (2 : 8 v/v), (b) THF–water (3 : 7 v/v) and (c) THF–water (4 : 6 v/v) solutions in the dark. The arrows indicate the spectral changes with time. The time intervals between every two spectra were 0.5 hour; (d) absorbance traces of compound **4** in THF–water mixed solutions at the absorption maximum with time at 293 K ([**4**] = 4×10^{-5} M).

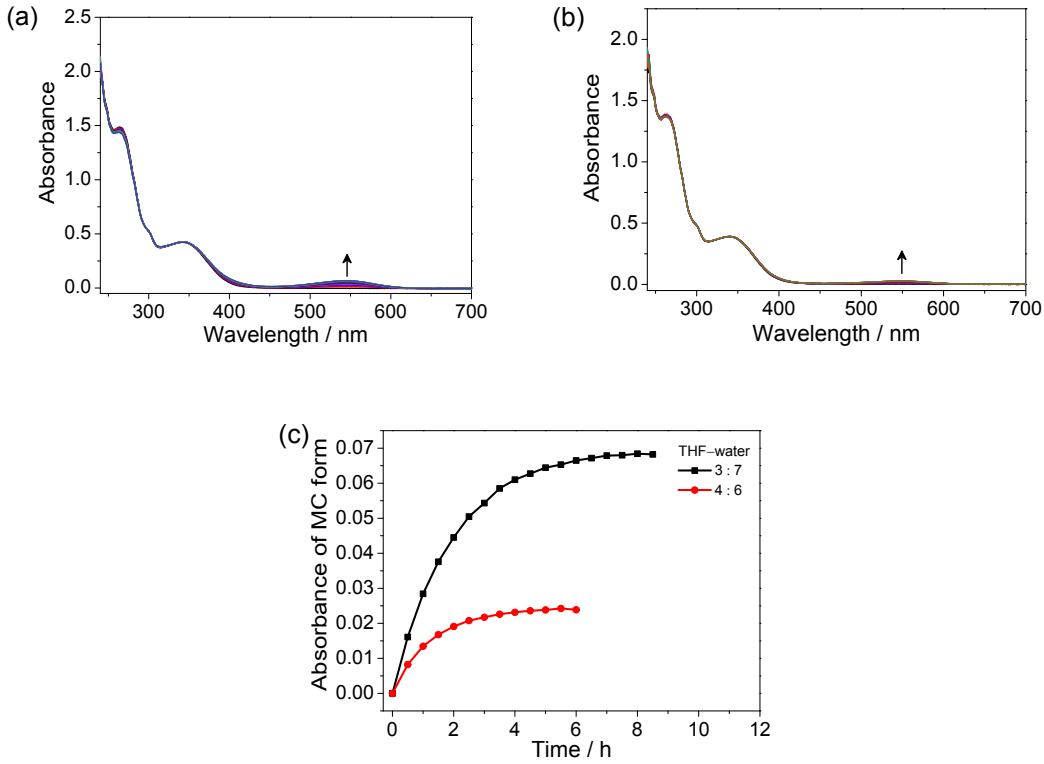

Figure S12. Time-dependent UV–vis absorption spectral changes of the closed form of compound **6** in (a) THF–water (3 : 7 v/v) and (b) THF–water (4 : 6 v/v) solutions in the dark. The arrows indicate the spectral changes with time. The time intervals between every two spectra were 0.5 hour; (c) absorbance traces of compound **6** in THF–water mixed solutions at the absorption maximum with time at 293 K ([**6**] = 4×10^{-5} M).

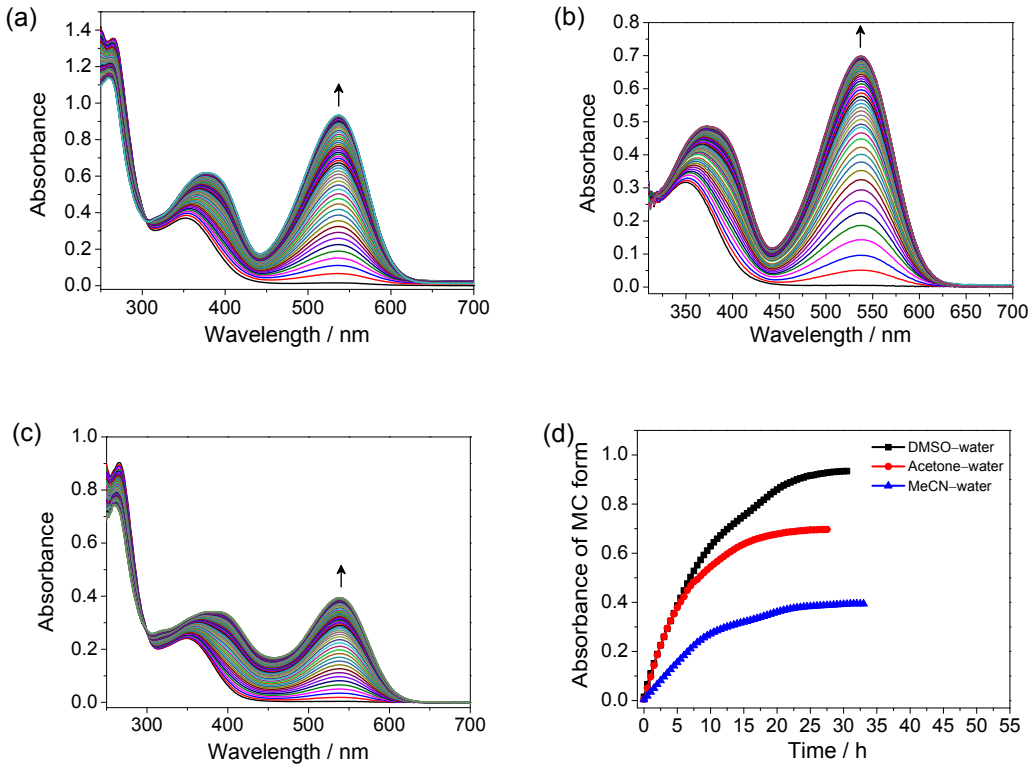

Figure S13. Time-dependent UV–vis absorption spectral changes of the closed form of compound **5** in (a) DMSO–water (1 : 4 v/v), (b) acetone–water (1 : 4 v/v) and (c) MeCN–water (1 : 4 v/v) solutions in the dark. The arrows indicate the spectral changes with time. The time intervals between every two spectra were 0.5 hour; (d) absorbance traces of compound **5** in mixed solutions at the absorption maximum with time at 293 K ([**5**] = 4×10^{-5} M).

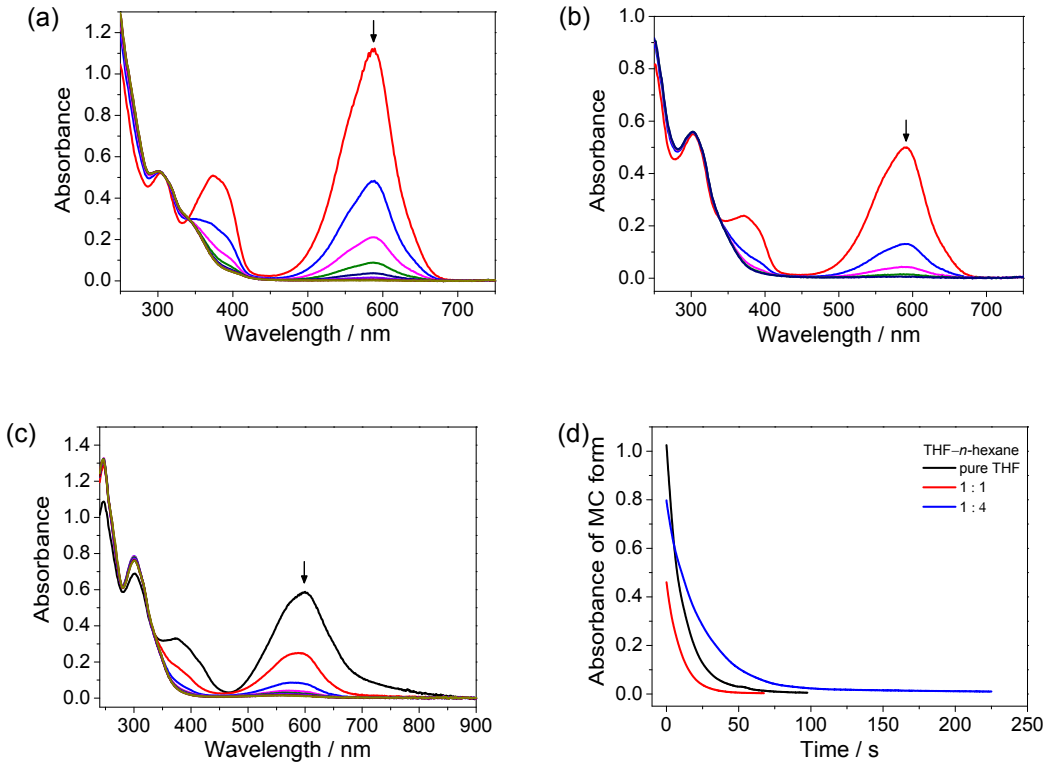

Figure S14. Time-dependent UV–vis absorption spectral changes of the open form of compound **1** in (a) THF, (b) THF–*n*-hexane (1 : 1 v/v) and (c) THF–*n*-hexane (1 : 4 v/v) solutions after excitation at 365 nm at 293 K. The arrows indicate the spectral changes with time. The time intervals between every two spectra were 30 seconds; (d) Decay traces at the absorption maximum with time at 293 K ([**1**] = 4×10^{-5} M).

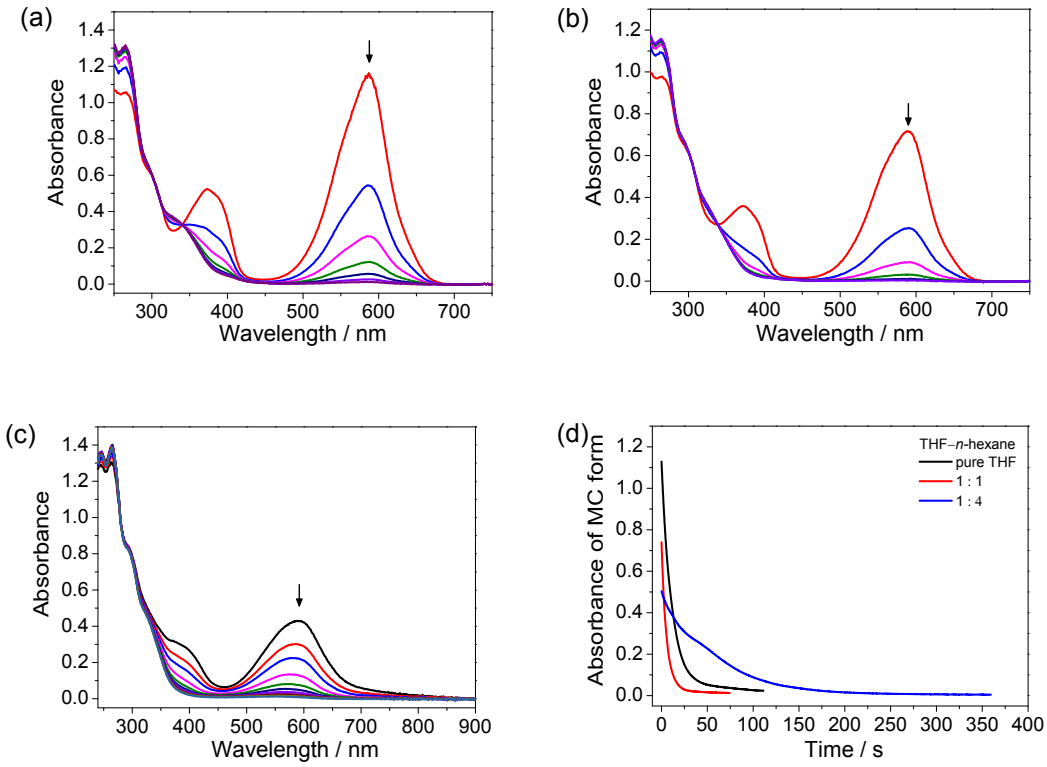

Figure S15. Time-dependent UV–vis absorption spectral changes of the open form of compound **2** in (a) THF, (b) THF–*n*-hexane (1 : 1 v/v) and (c) THF–*n*-hexane (1 : 4 v/v) solutions after excitation at 365 nm at 293 K. The arrows indicate the spectral changes with time. The time intervals between every two spectra were 30 seconds; (d) Decay traces at the absorption maximum with time at 293 K ([**2**] = 4×10^{-5} M).

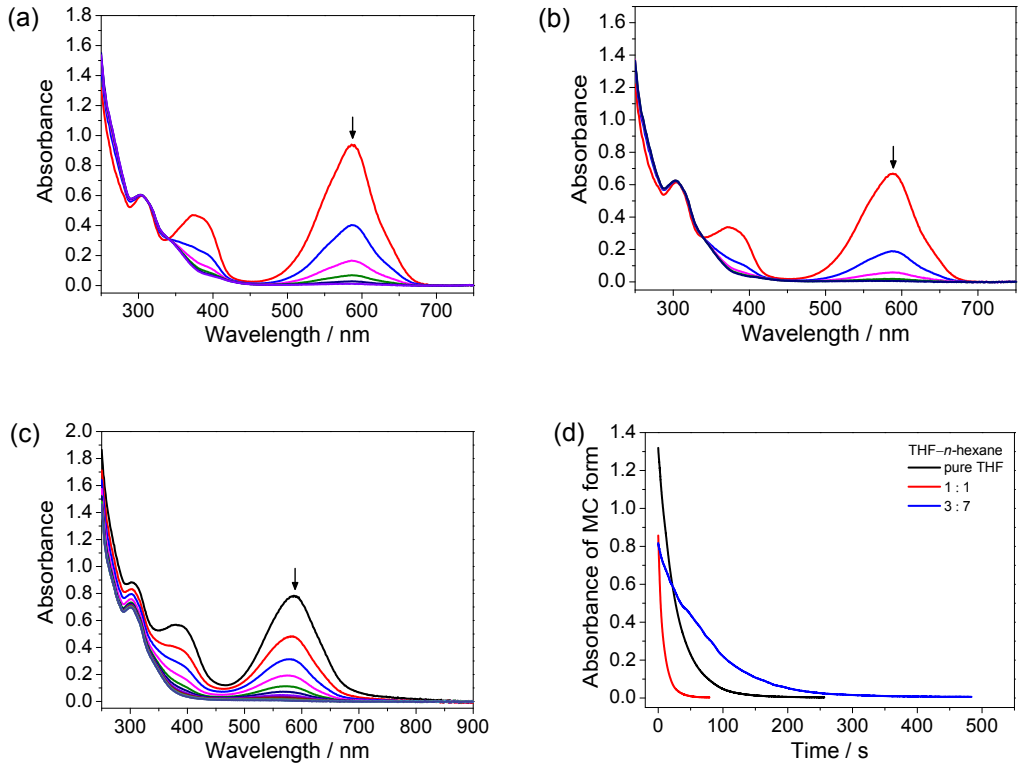

Figure S16. Time-dependent UV–vis absorption spectral changes of the open form of compound **3** in (a) THF, (b) THF–*n*-hexane (1 : 1 v/v) and (c) THF–*n*-hexane (3 : 7 v/v) solutions after excitation at 365 nm at 293 K. The arrows indicate the spectral changes with time. The time intervals between every two spectra were 30 seconds; (d) Decay traces at the absorption maximum with time at 293 K ([**3**] = 4×10^{-5} M).

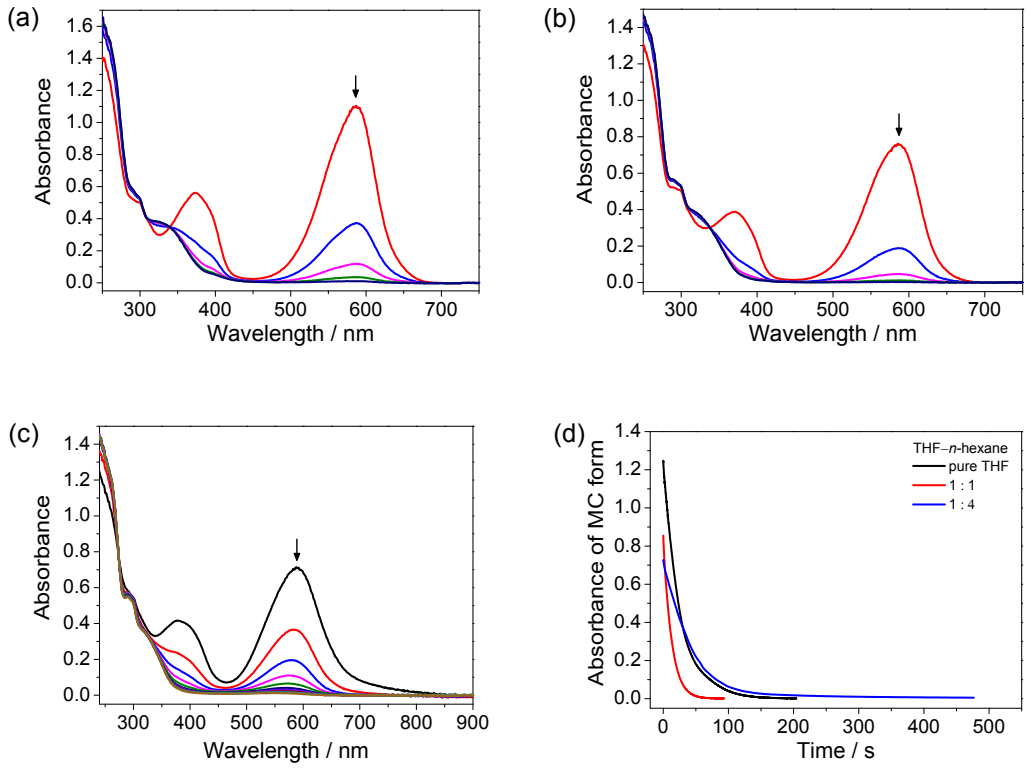

Figure S17. Time-dependent UV–vis absorption spectral changes of the open form of compound **4** in (a) THF, (b) THF–*n*-hexane (1 : 1 v/v) and (c) THF–*n*-hexane (1 : 4 v/v) solutions after excitation at 365 nm at 293 K. The arrows indicate the spectral changes with time. The time intervals between every two spectra were 30 seconds; (d) Decay traces at the absorption maximum with time at 293 K ([**4**] = 4×10^{-5} M).

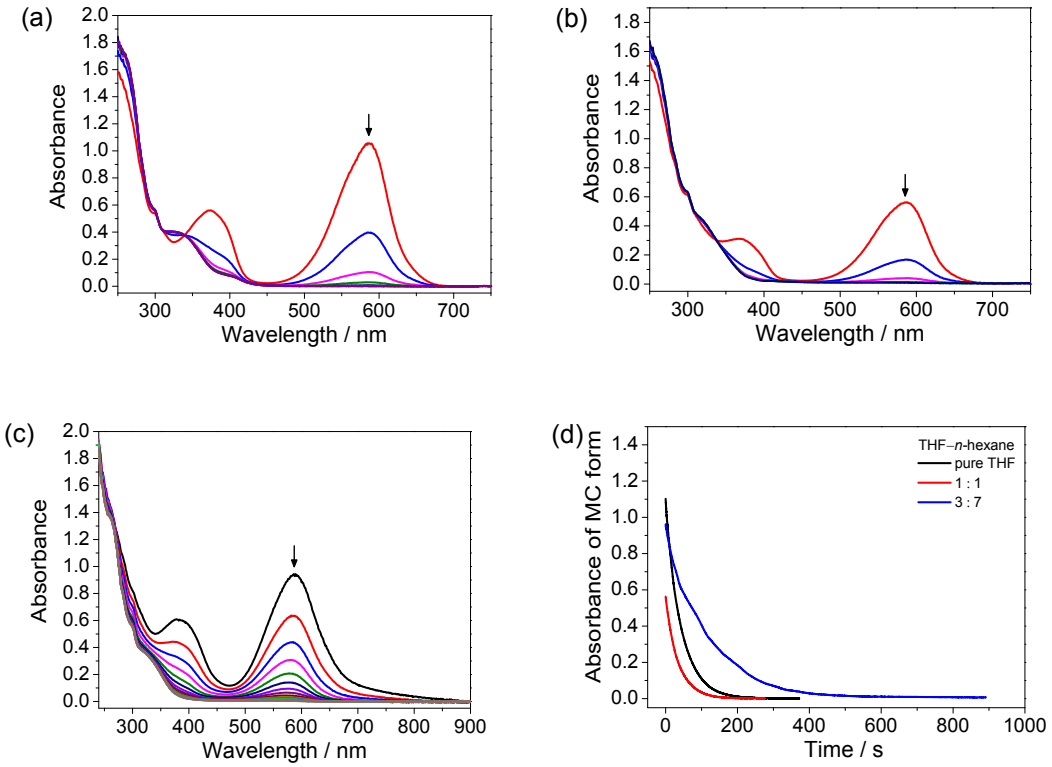

Figure S18. Time-dependent UV–vis absorption spectral changes of the open form of compound **6** in (a) THF, (b) THF–*n*-hexane (1 : 1 v/v) and (c) THF–*n*-hexane (3 : 7 v/v) solutions after excitation at 365 nm at 293 K. The arrows indicate the spectral changes with time. The time intervals between every two spectra were 30 seconds; (d) Decay traces at the absorption maximum with time at 293 K ([**6**] = 4×10^{-5} M).

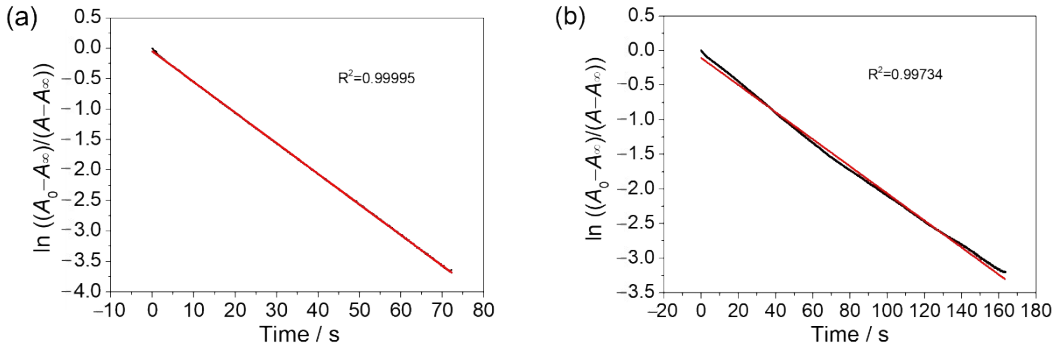

Figure S19. Plots of ln $[(A - A_\infty)/(A_0 - A_\infty)]$ against t from the bleaching reaction of compound **5** in (a) THF and (b) THF–*n*-hexane (1 : 4 v/v) at 298 K ([**5**] = 4×10^{-5} M).

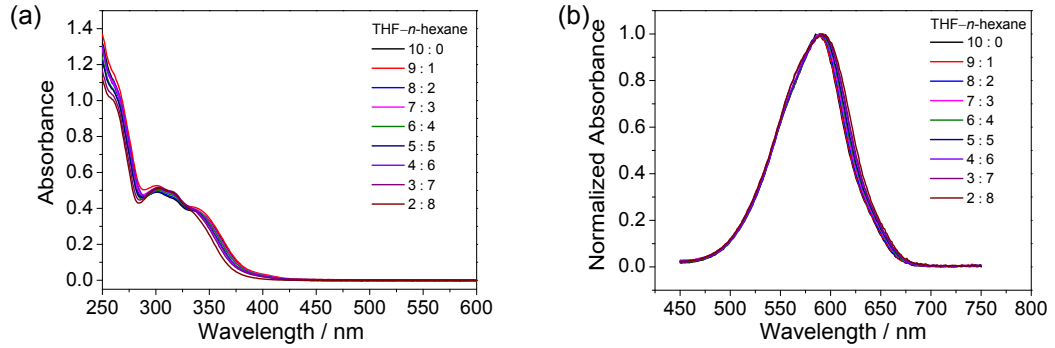

Figure S20. (a) UV−Vis absorption spectra of compound **1** in closed form and (b) normalized UV–vis absorption spectra of compound **1** after irradiation with UV light in THF solutions upon increasing *n*-hexane content from 0 to 80 % ([**1**] = 4×10^{-5} M).

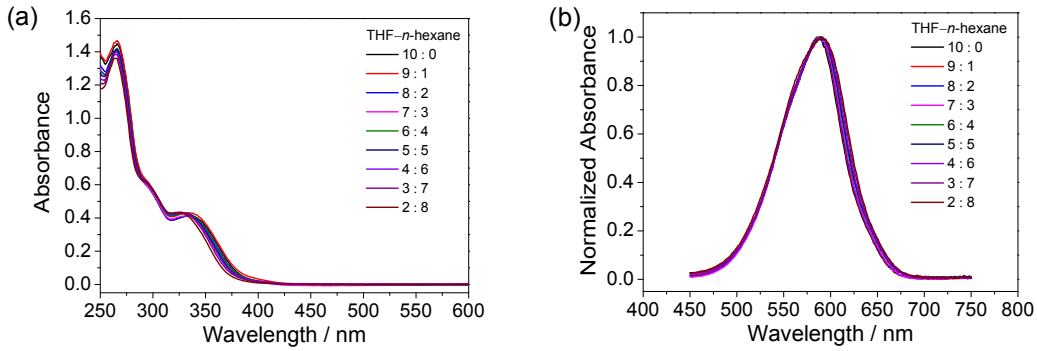

Figure S21. (a) UV−Vis absorption spectra of compound **2** in closed form and (b) normalized UV−vis absorption spectra of compound **2** after irradiation with UV light in THF solutions upon increasing *n*-hexane content from 0 to 80 % ([**2**] = 4×10^{-5} M).

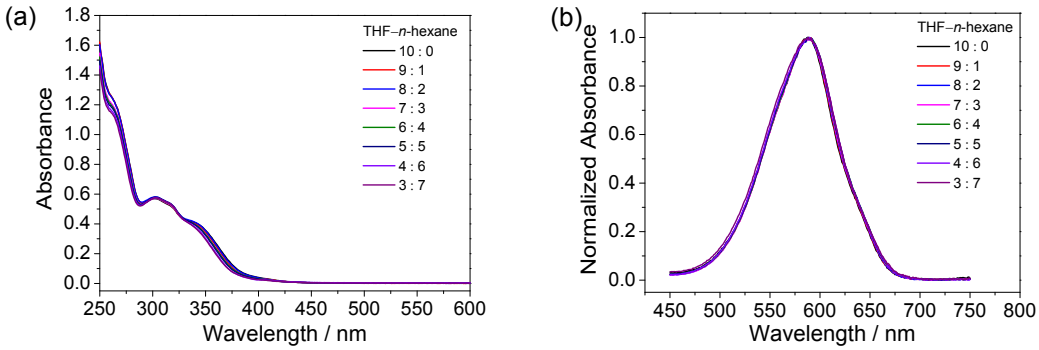

Figure S22. (a) UV−Vis absorption spectra of compound **3** in closed form and (b) normalized UV−vis absorption spectra of compound **3** after irradiation with UV light in THF solutions upon increasing *n*-hexane content from 0 to 70 % ([**3**] = 4×10^{-5} M).

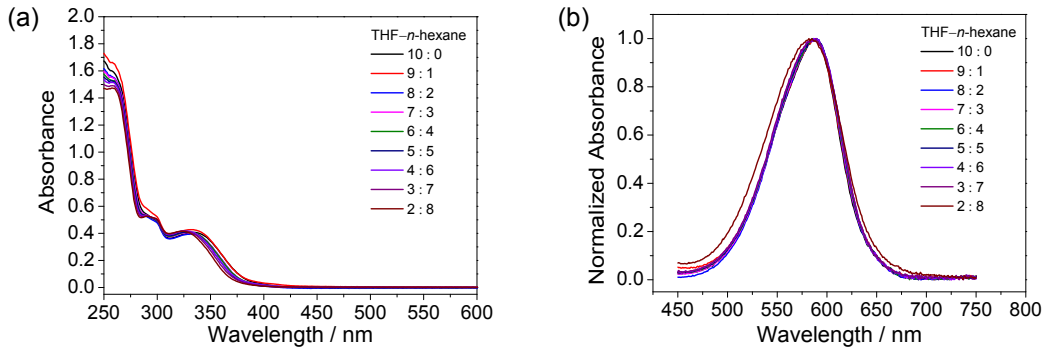

Figure S23. (a) UV−Vis absorption spectra of compound **4** in closed form and (b) normalized UV−vis absorption spectra of compound **4** after irradiation with UV light in THF solutions upon increasing *n*-hexane content from 0 to 80 % ([**4**] = 4×10^{-5} M).

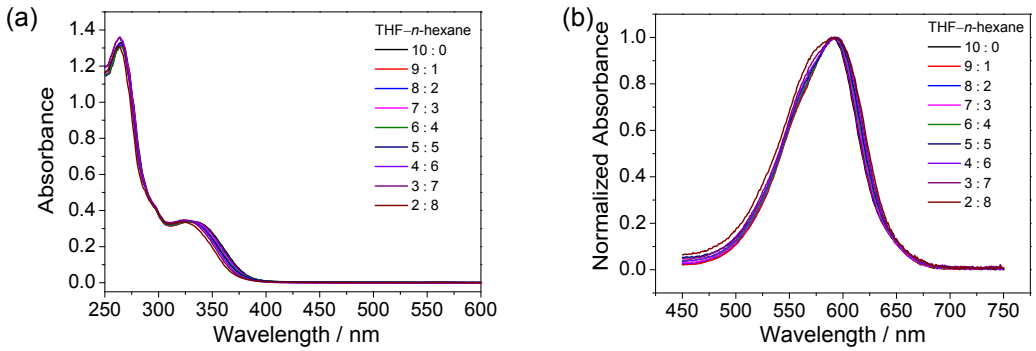

Figure S24. (a) UV−Vis absorption spectra of compound **5** in closed form and (b) normalized UV−vis absorption spectra of compound **5** after irradiation with UV light in THF solutions upon increasing *n*-hexane content from 0 to 80 % ([**5**] = 4×10^{-5} M).

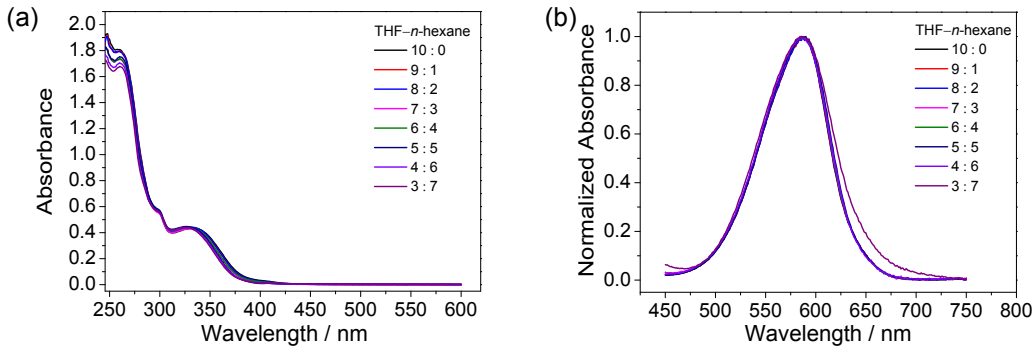

Figure S25. (a) UV−Vis absorption spectra of compound **6** in closed form and (b) normalized UV–vis absorption spectra of compound **6** after irradiation with UV light in THF solutions upon increasing *n*-hexane content from 0 to 70 % ([**6**] = 4×10^{-5} M).

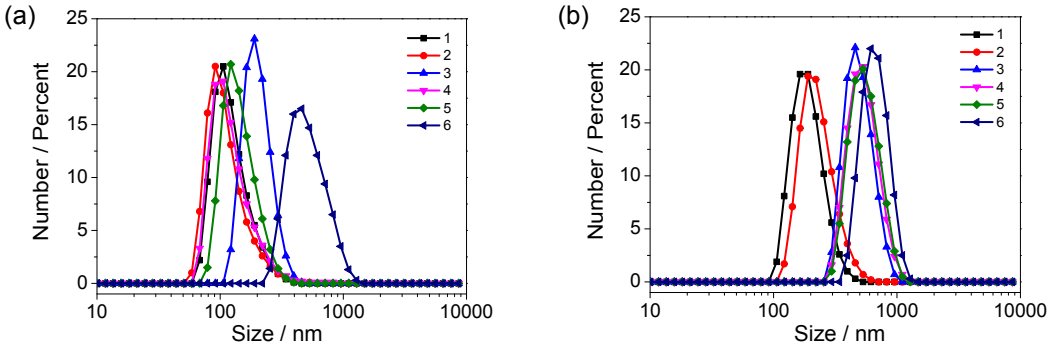

Figure S26. DLS results of compounds **1**–**6** in THF–*n*-hexane (1 : 4 v/v) for compounds **1**, **2**, **4** and **5** and THF–*n*-hexane (3 : 7 v/v) for compounds **3** and **6** (a) before and (b) after UV irradiation (conc = 4×10^{-5} M).

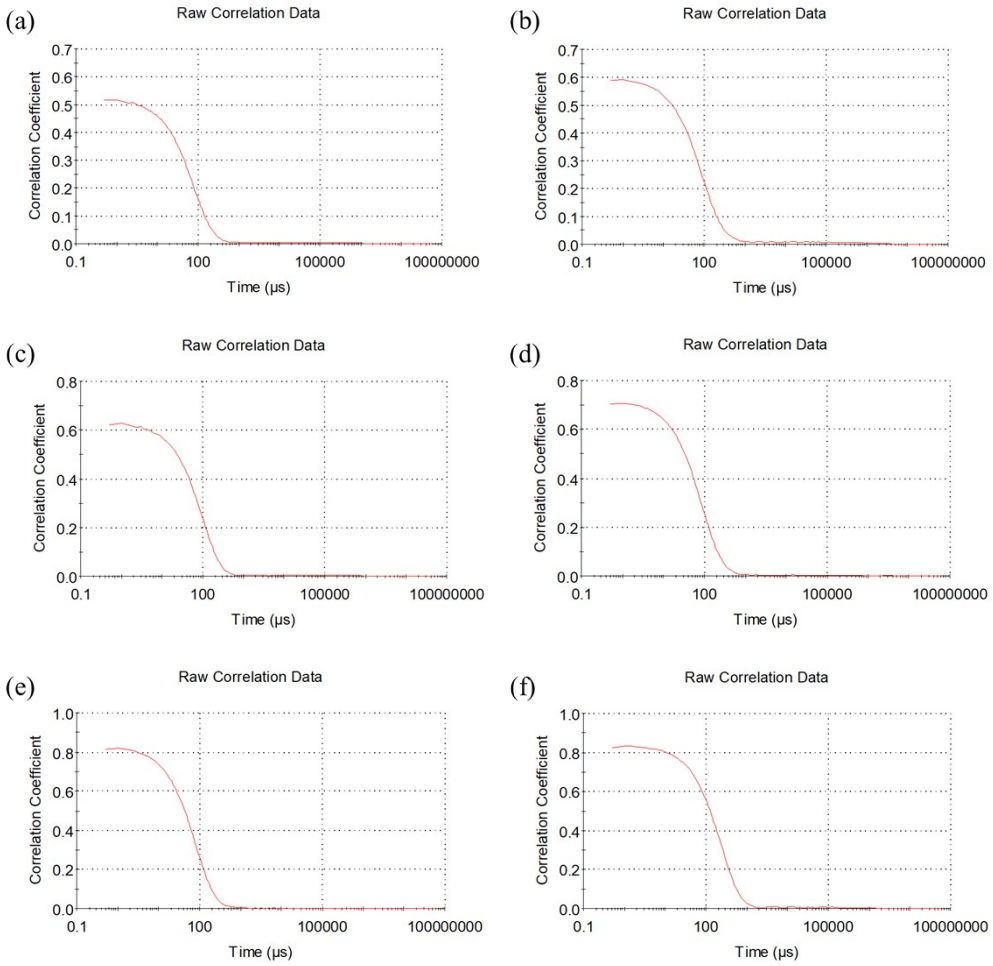

Figure S27. The autocorrelation function of the DLS results of compounds **1**–**6** (a–f) in THF–*n*-hexane (1 : 4 v/v) for compounds **1**, **2**, **4** and **5** and THF–*n*-hexane (3 : 7 v/v) for compounds **3** and **6** before UV irradiation (conc = 4×10^{-5} M).

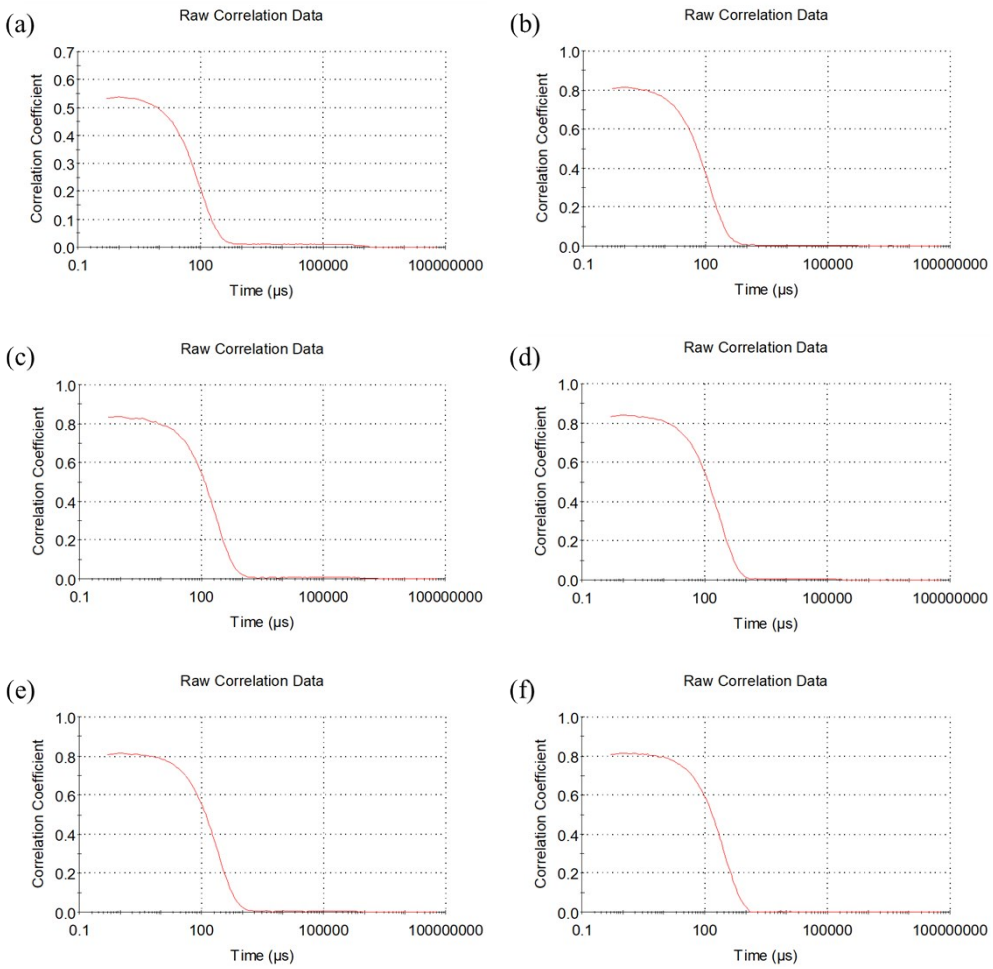

Figure S28. The autocorrelation function of the DLS results of compounds **1**–**6** (a–f) in THF–*n*-hexane (1 : 4 v/v) for compounds **1**, **2**, **4** and **5** and THF–*n*-hexane (3 : 7 v/v) for compounds **3** and **6** after UV irradiation (conc = 4×10^{-5} M).

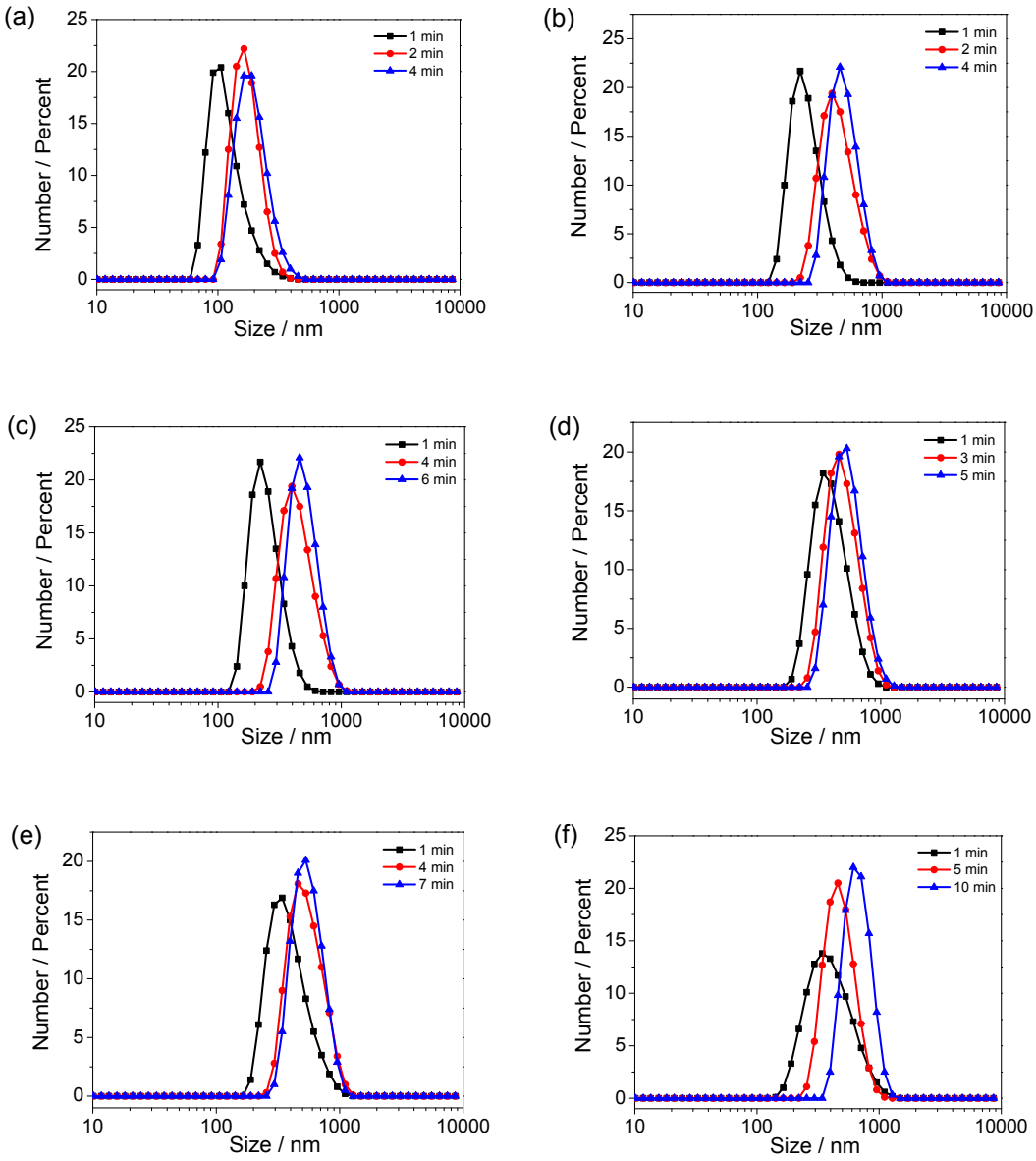

Figure S29. Time-dependent DLS experiments of compounds **1**–**6** (a–f) in THF–*n*-hexane (1 : 4 v/v) for compounds **1**, **2**, **4** and **5** and THF–*n*-hexane (3 : 7 v/v) for compounds **3** and **6** upon UV irradiation for various time interval (conc = 4×10^{-5} M).

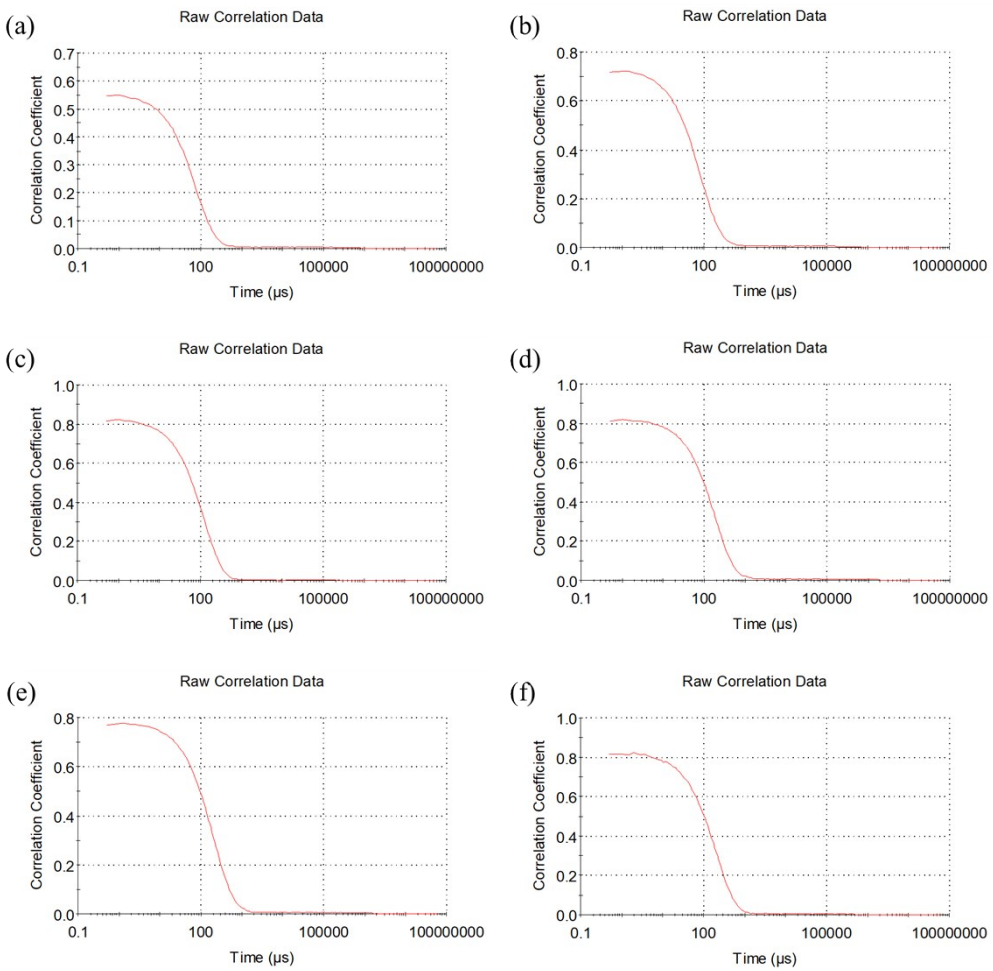

Figure S30. The autocorrelation function of the DLS results of compounds **1**–**6** (a–f) in THF–*n*-hexane (1 : 4 v/v) for compounds **1**, **2**, **4** and **5** and THF–*n*-hexane (3 : 7 v/v) for compounds **3** and **6** after UV irradiation at a stand time of 1 min (conc = 4×10^{-5} M).

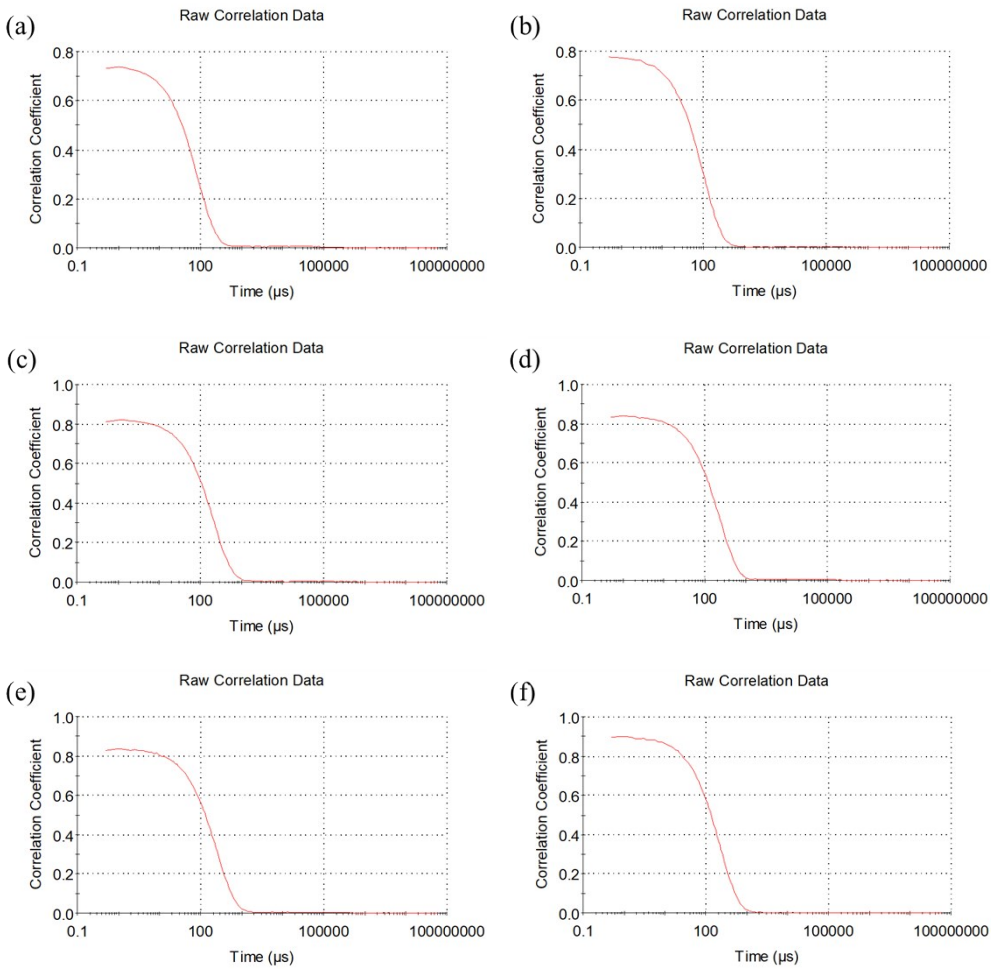

Figure S31. The autocorrelation function of the DLS results of compounds **1**–**6** (a–f) in THF–*n*-hexane (1 : 4 v/v) for compounds **1**, **2**, **4** and **5** and THF–*n*-hexane (3 : 7 v/v) for compounds **3** and **6** after UV irradiation at different stand time (2 min for **1**, 2 min for **2**, 4 min for **3**, 3 min for **4**, 4 min for **5** and 5 min for **6**) (conc = 4×10^{-5} M).

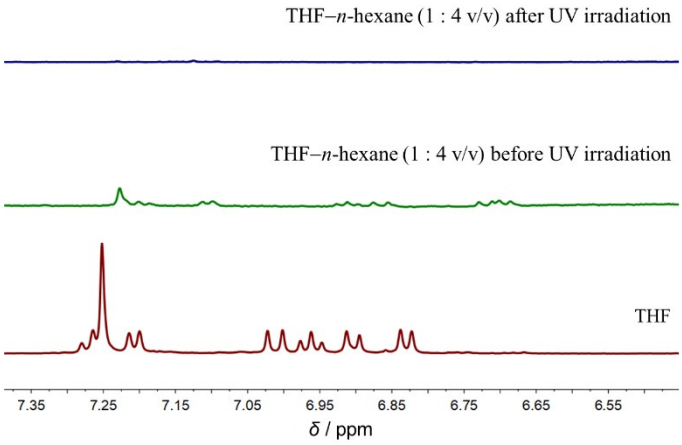

Figure S32. ^{1}H NMR spectra of compound **5** in THF solution and THF–*n*-hexane (1 : 4 v/v) solution before and after UV light irradiation (conc = 4×10^{-5} M).

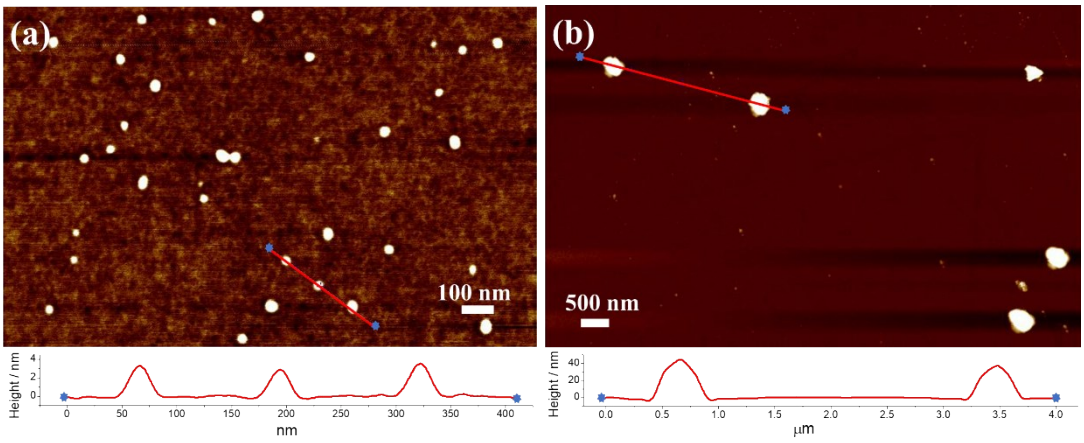

Figure S33. AFM images prepared from compound **5** in THF–*n*-hexane (1 : 4 v/v) (a) before and (b) after UV irradiation ([**5**] = 4×10^{-5} M).

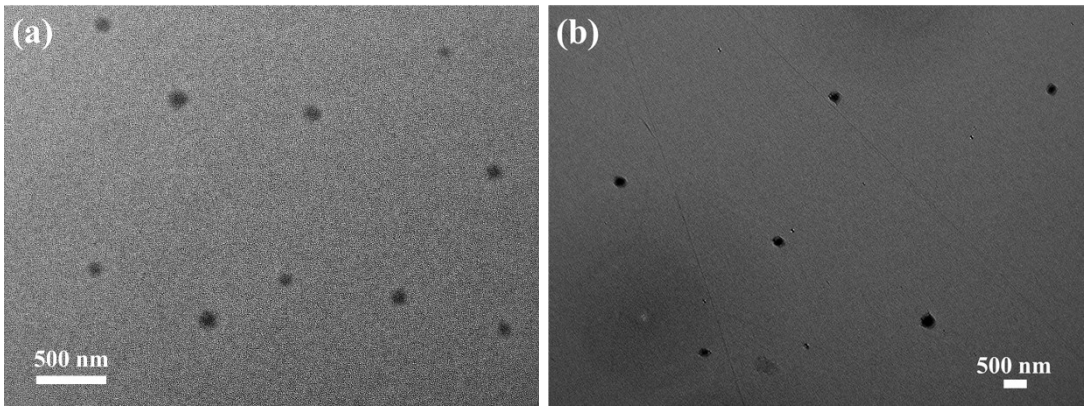

Figure S34. TEM images prepared from compound **1** in THF–*n*-hexane (1 : 4 v/v) (a) before and (b) after UV irradiation ([**1**] = 4×10^{-5} M).

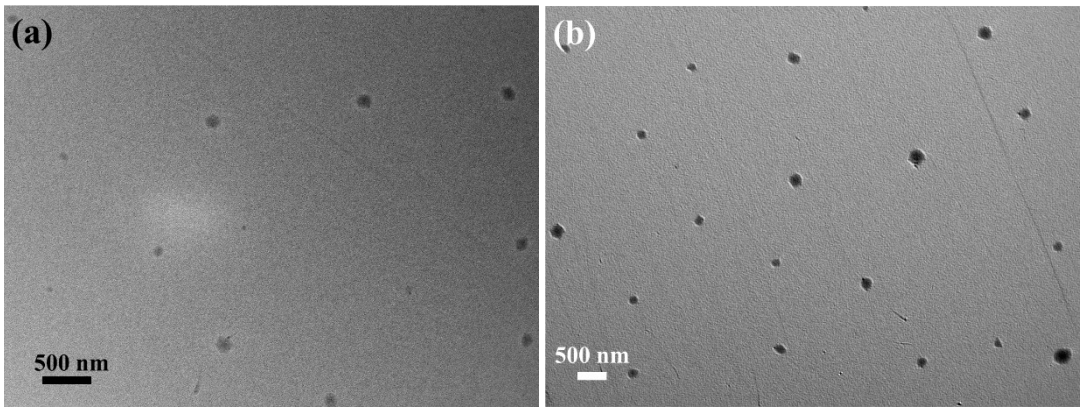

Figure S35. TEM images prepared from compound **2** in THF–*n*-hexane (1 : 4 v/v) (a) before and (b) after UV irradiation ([**2**] = 4×10^{-5} M).

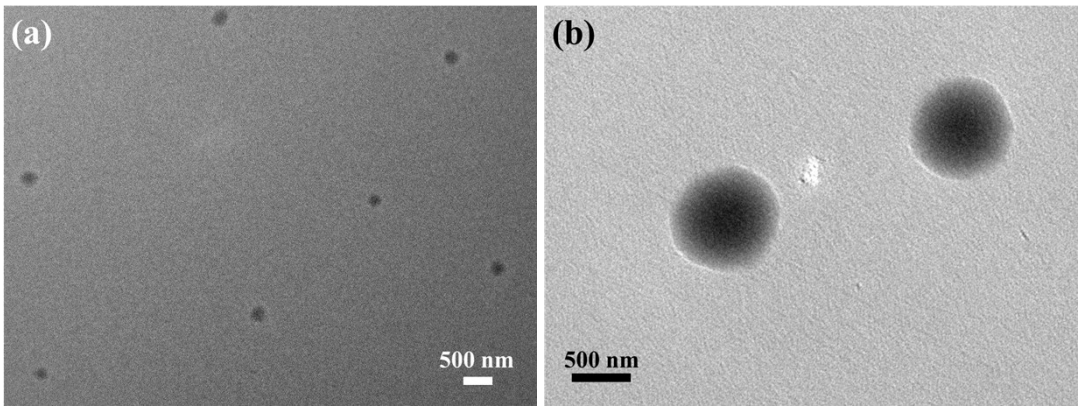

Figure S36. TEM images prepared from compound **3** in THF–*n*-hexane (3 : 7 v/v) (a) before and (b) after UV irradiation ([**3**] = 4×10^{-5} M).

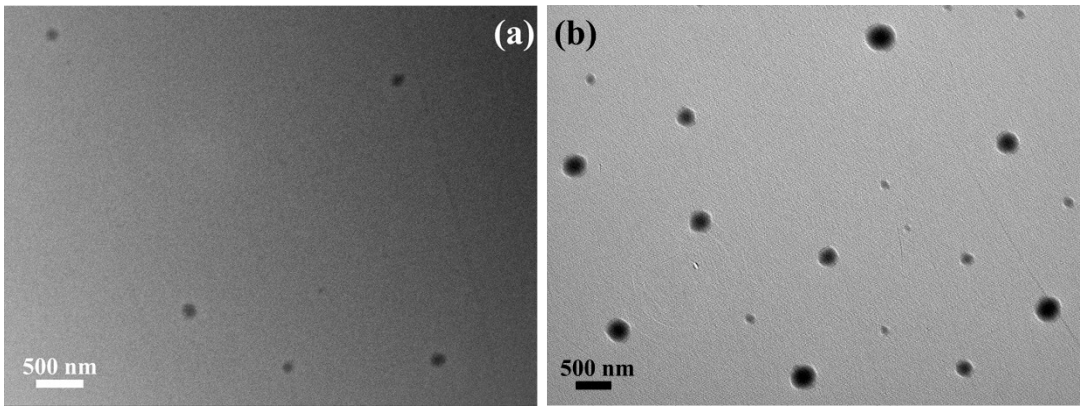

Figure S37. TEM images prepared from compound **4** in THF–*n*-hexane (1 : 4 v/v) (a) before and (b) after UV irradiation ([**4**] = 4×10^{-5} M).

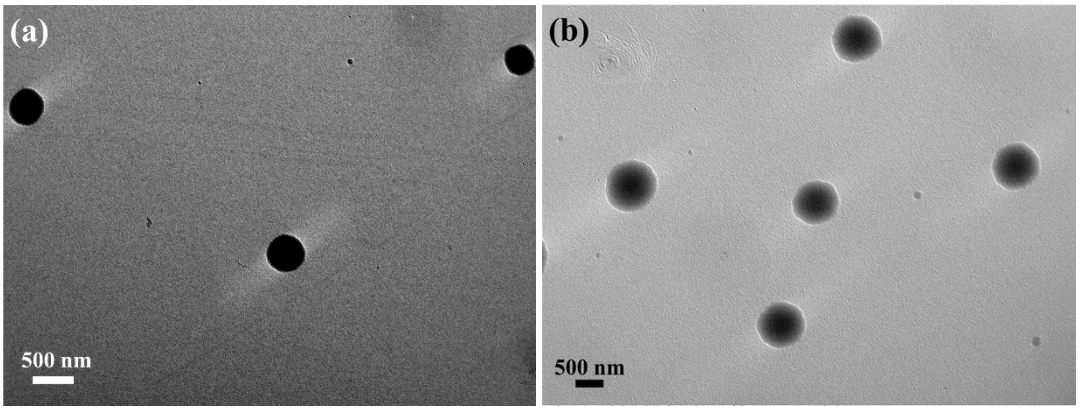

Figure S38. TEM images prepared from compound **6** in THF–*n*-hexane (3 : 7 v/v) (a) before and (b) after UV irradiation ([**6**] = 4×10^{-5} M).

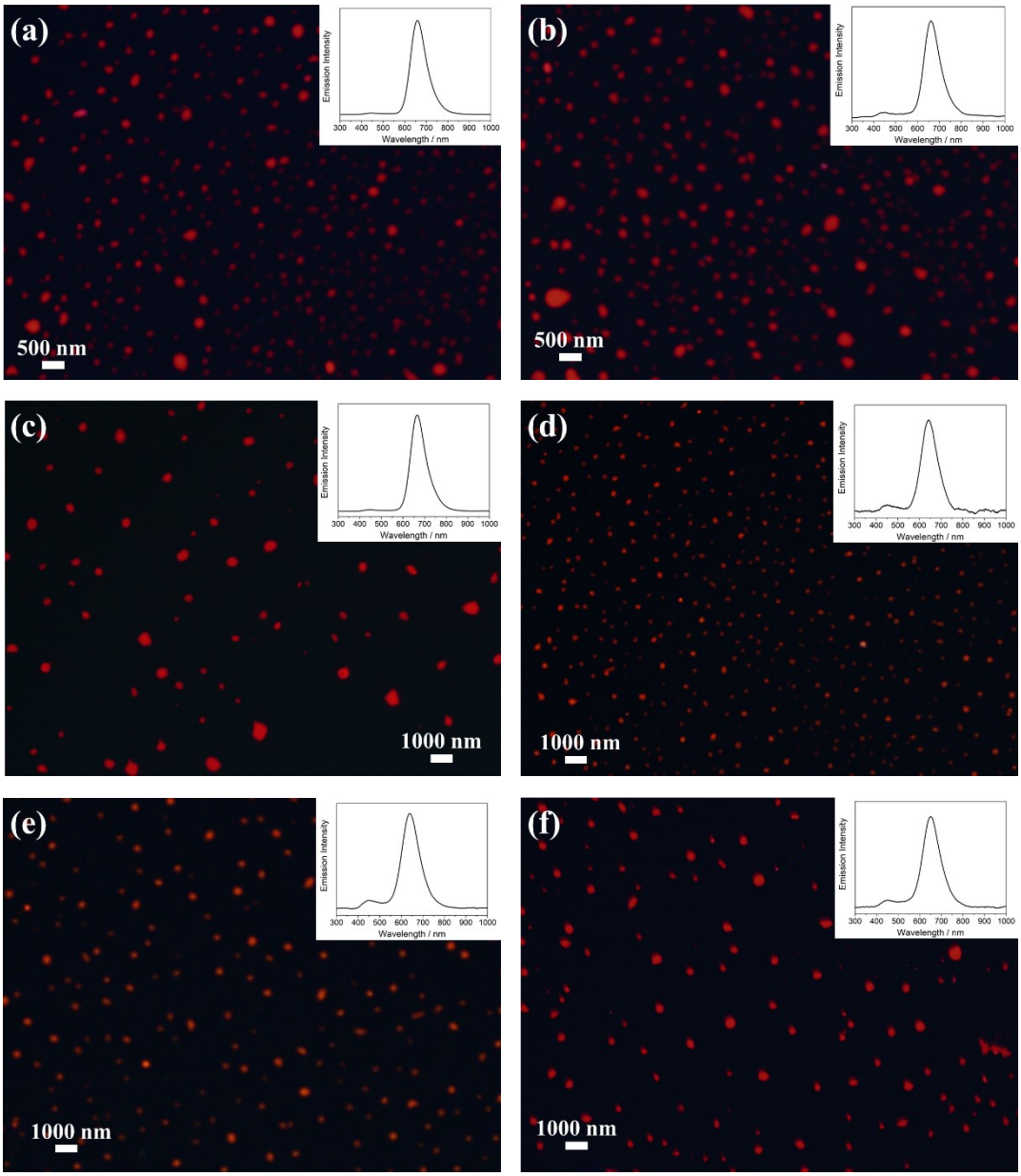

Figure S39. Fluorescence microscopy images of open forms of compounds **1**–**6** (a–f) in THF–*n*-hexane (1 : 4 v/v) for compounds **1**, **2**, **4** and **5** and THF–*n*-hexane (3 : 7 v/v) for compounds **3** and **6** at 288 K. Inset: *In situ* emission spectra (conc = 4×10^{-5} M).

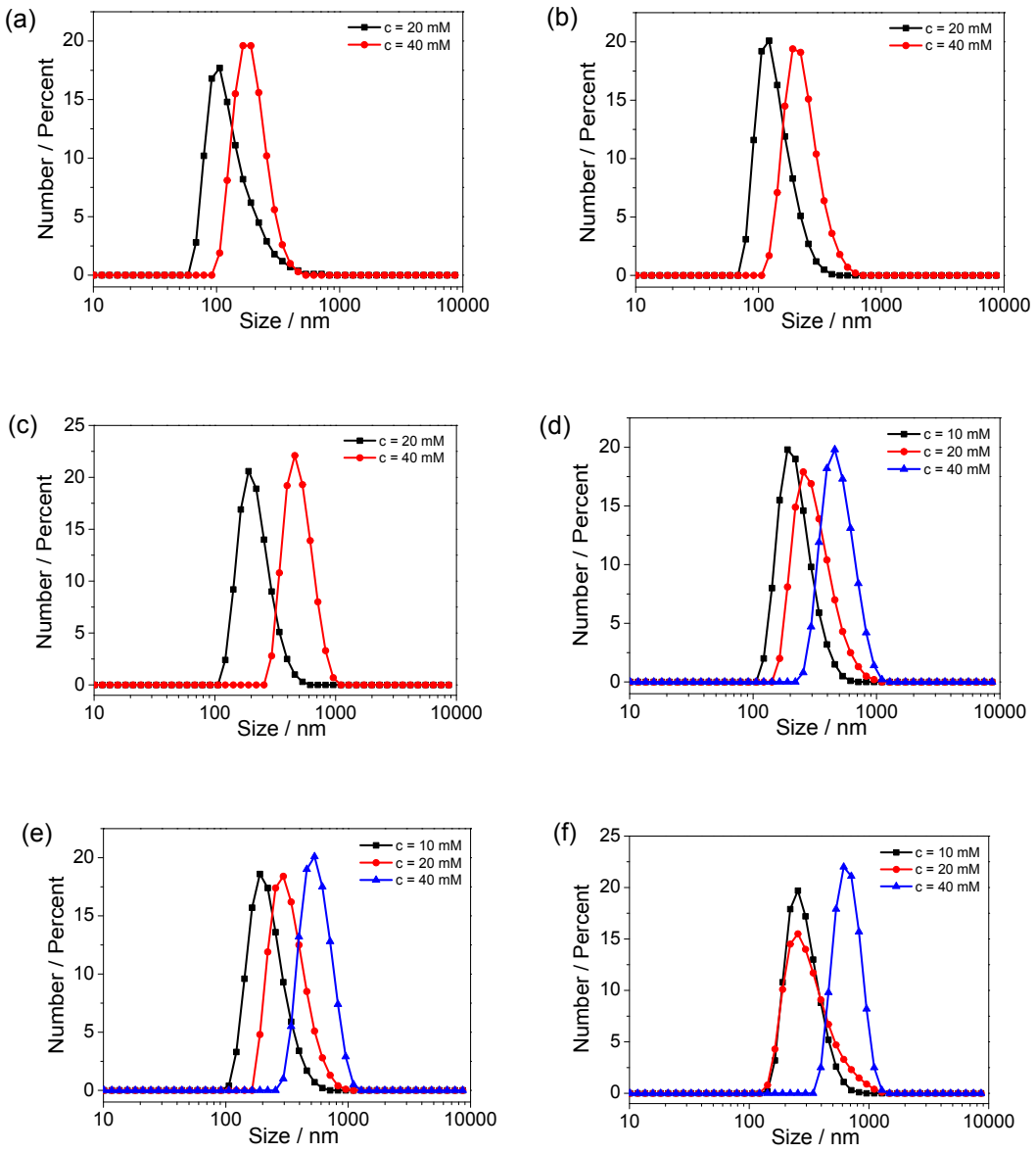

Figure S40. DLS results of compounds **1**–**6** (a–f) in THF–*n*-hexane (1 : 4 v/v) for compounds **1**, **2**, **4** and **5** and THF–*n*-hexane (3 : 7 v/v) for compounds **3** and **6** after UV irradiation at different concentrations.

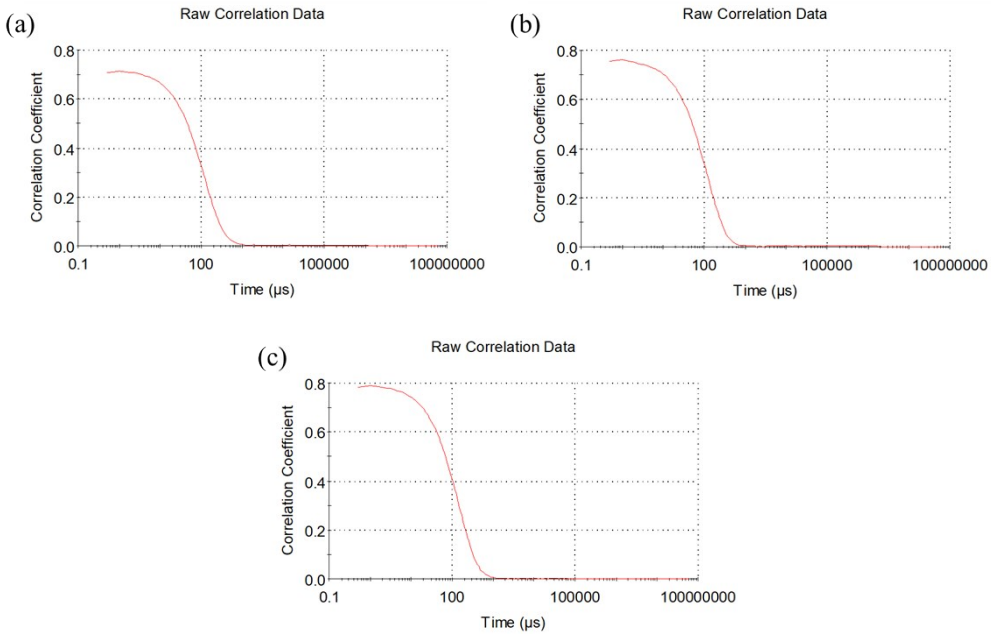

Figure S41. The autocorrelation function of the DLS results of compounds **4**–**6** (a–c) in THF–*n*-hexane (1 : 4 v/v) for compounds **4** and **5** and THF–*n*-hexane (3 : 7 v/v) for compounds **6** after UV irradiation (conc = 1×10^{-5} M).

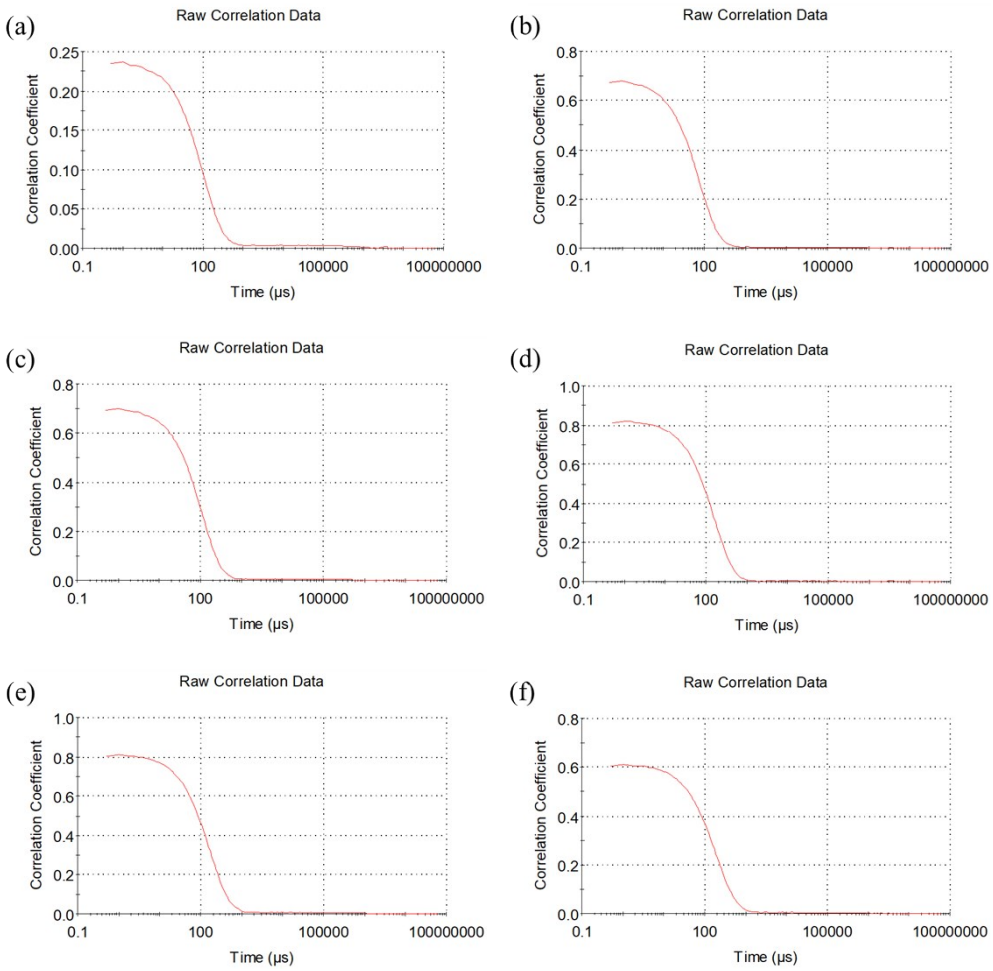

Figure S42. The autocorrelation function of the DLS results of compounds **1**–**6** (a–f) in THF–*n*-hexane (1 : 4 v/v) for compounds **1**, **2**, **4** and **5** and THF–*n*-hexane (3 : 7 v/v) for compounds **3** and **6** after UV irradiation (conc = 2×10^{-5} M).

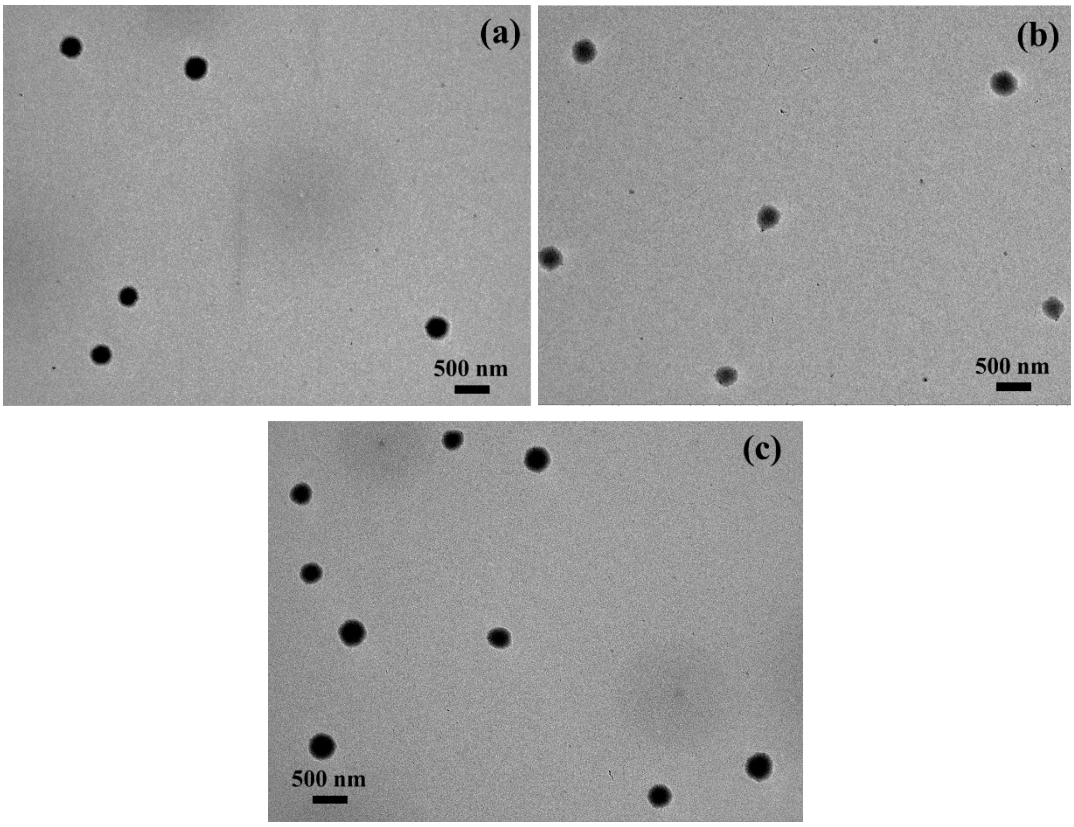

Figure S43. TEM images prepared from compounds **4**–**6** (a–c) in THF–*n*-hexane (1 : 4 v/v) for compounds **4** and **5** and THF–*n*-hexane (3 : 7 v/v) for compounds **6** after UV irradiation (conc = 1×10^{-5} M).

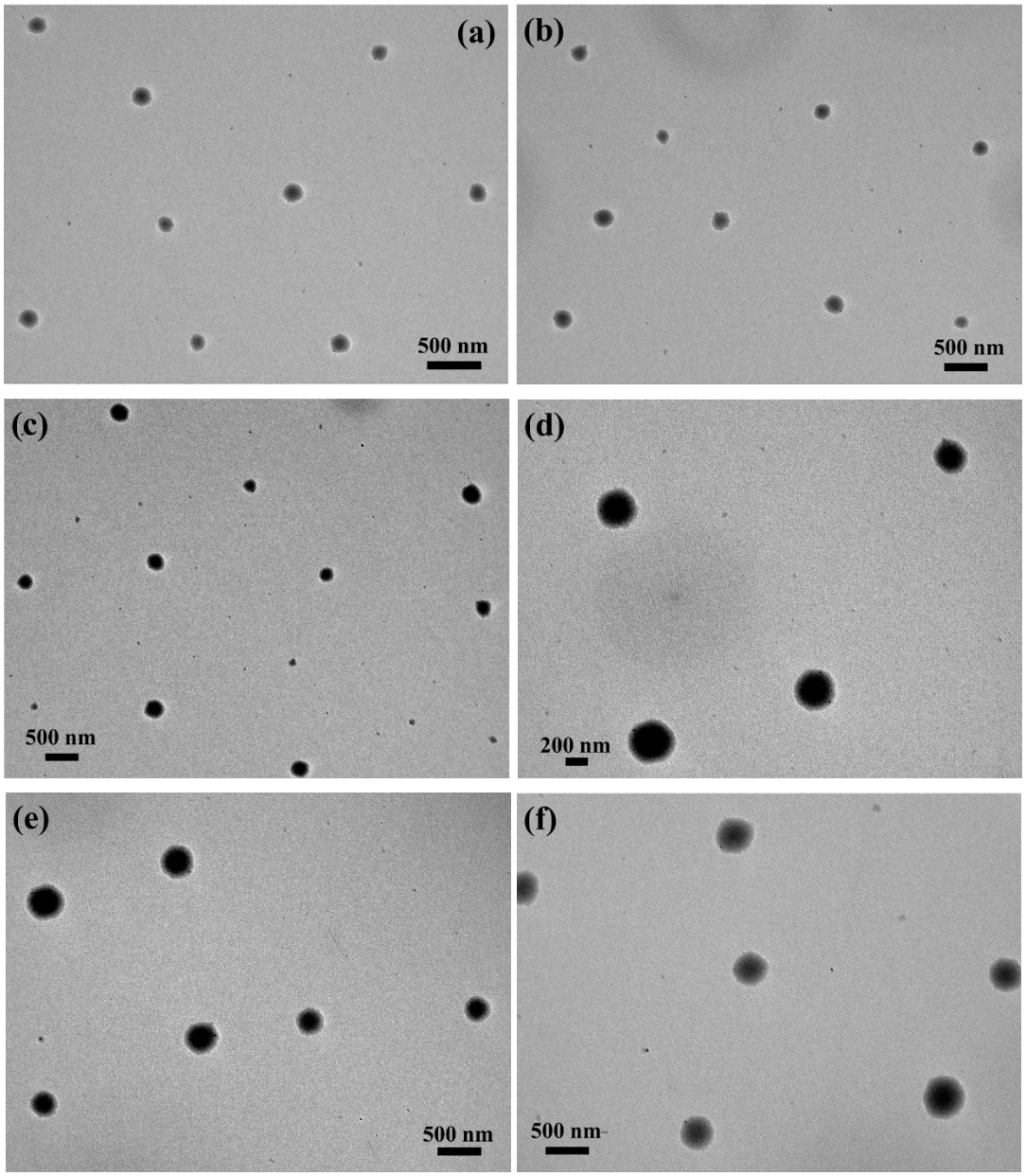

Figure S44. TEM images prepared from compounds **1**–**6** (a–f) in THF–*n*-hexane (1 : 4 v/v) for compounds **1**, **2**, **4** and **5** and THF–*n*-hexane (3 : 7 v/v) for compounds **3** and **6** after UV irradiation (conc = 2×10^{-5} M).

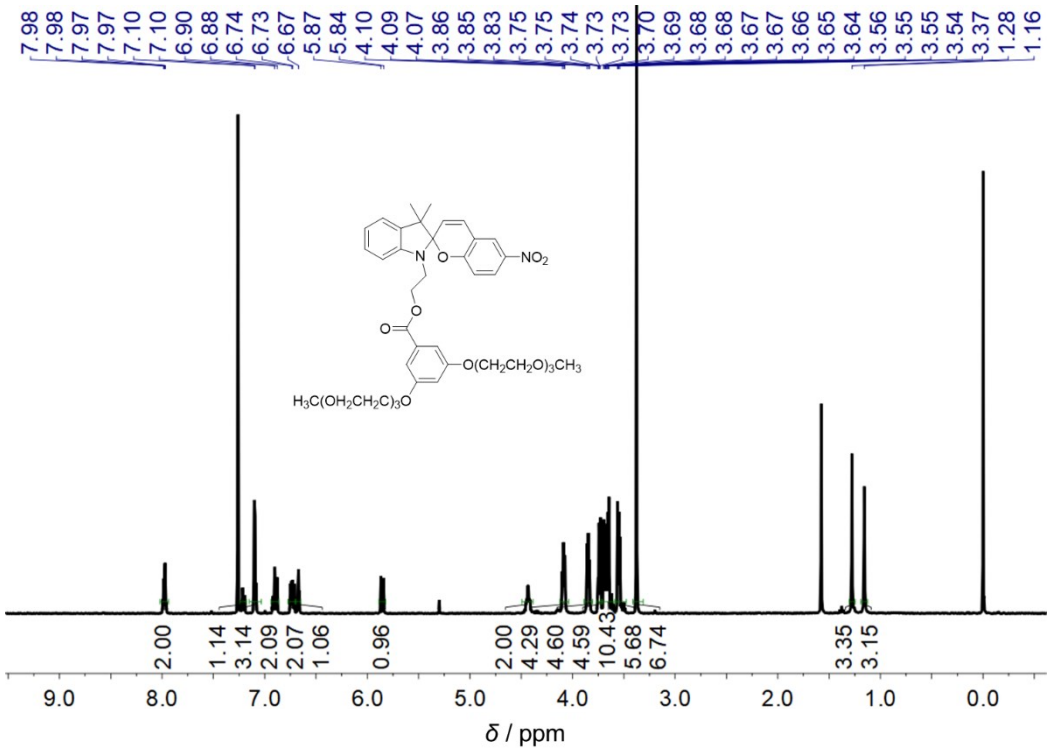

Figure S45. ^{1}H NMR spectrum of compound **1** in $CDCl_3$ at room temperature.

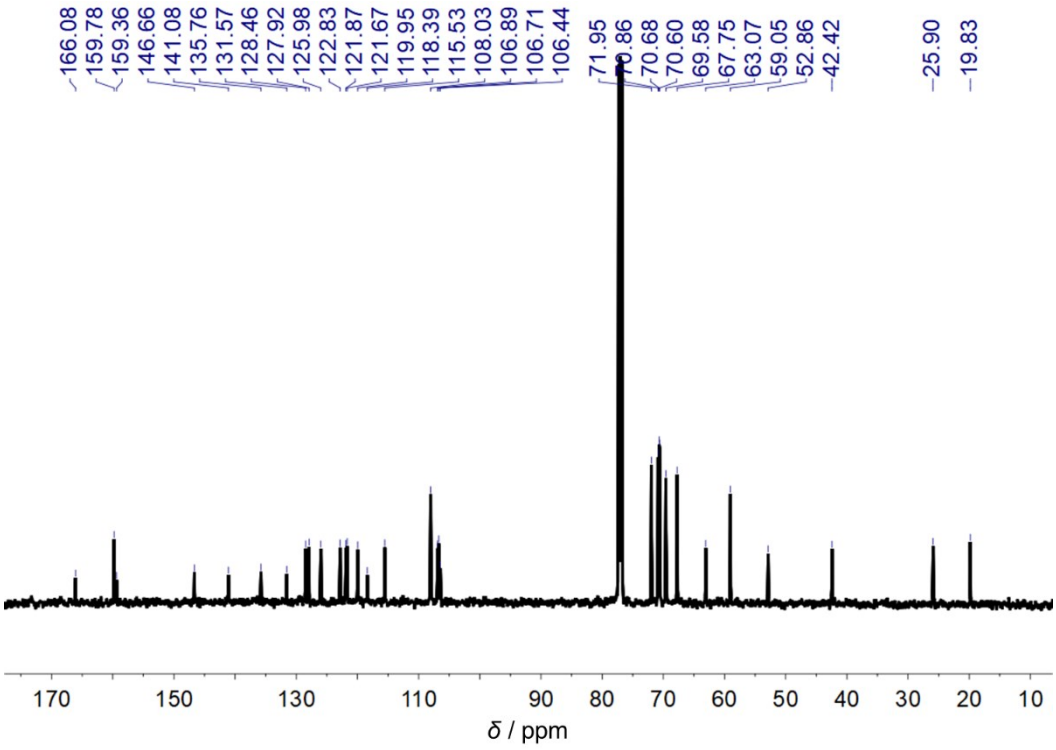

Figure S46. $^{13}C\{^{1}H\}$ NMR spectrum of compound **1** in $CDCl_3$ at room temperature.

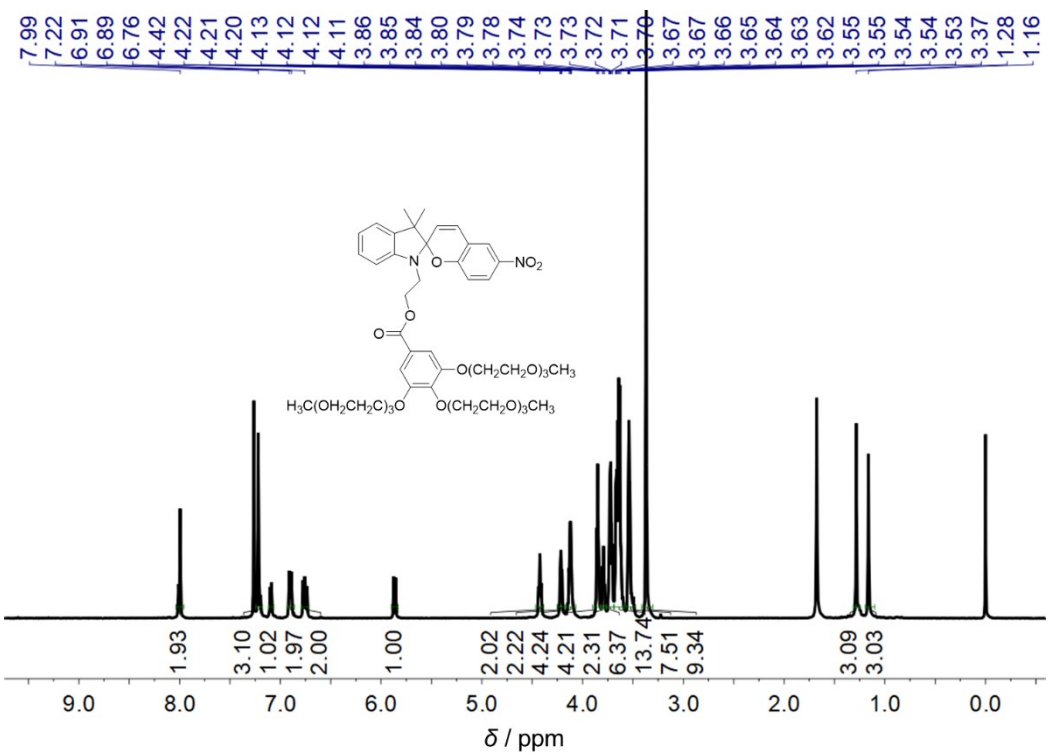

Figure S47. ^{1}H NMR spectrum of compound **2** in $CDCl_3$ at room temperature.

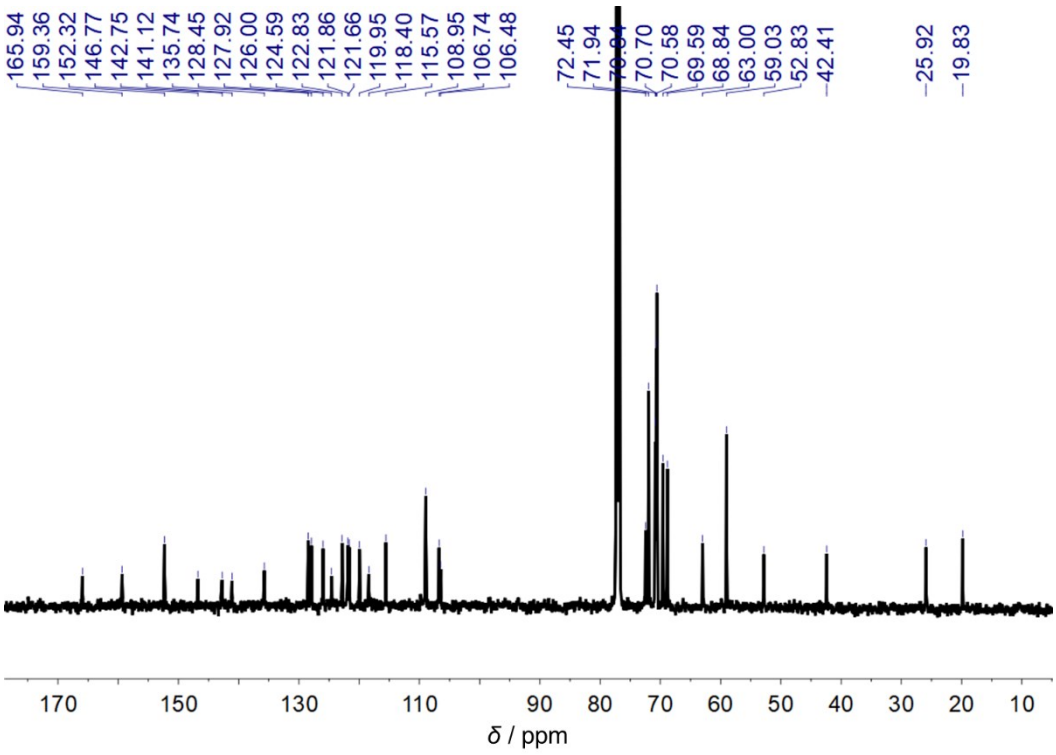

Figure S48. $^{13}C\{^{1}H\}$ NMR spectrum of compound **2** in $CDCl_3$ at room temperature.

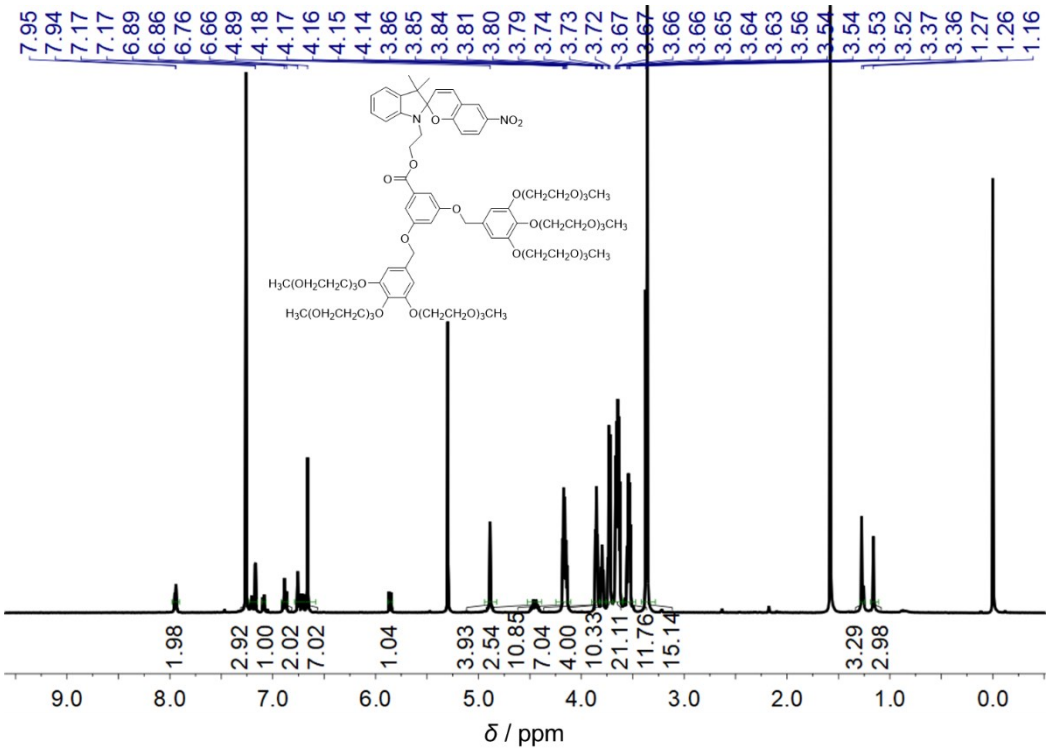

Figure S49. ^{1}H NMR spectrum of compound **3** in $CDCl_3$ at room temperature.

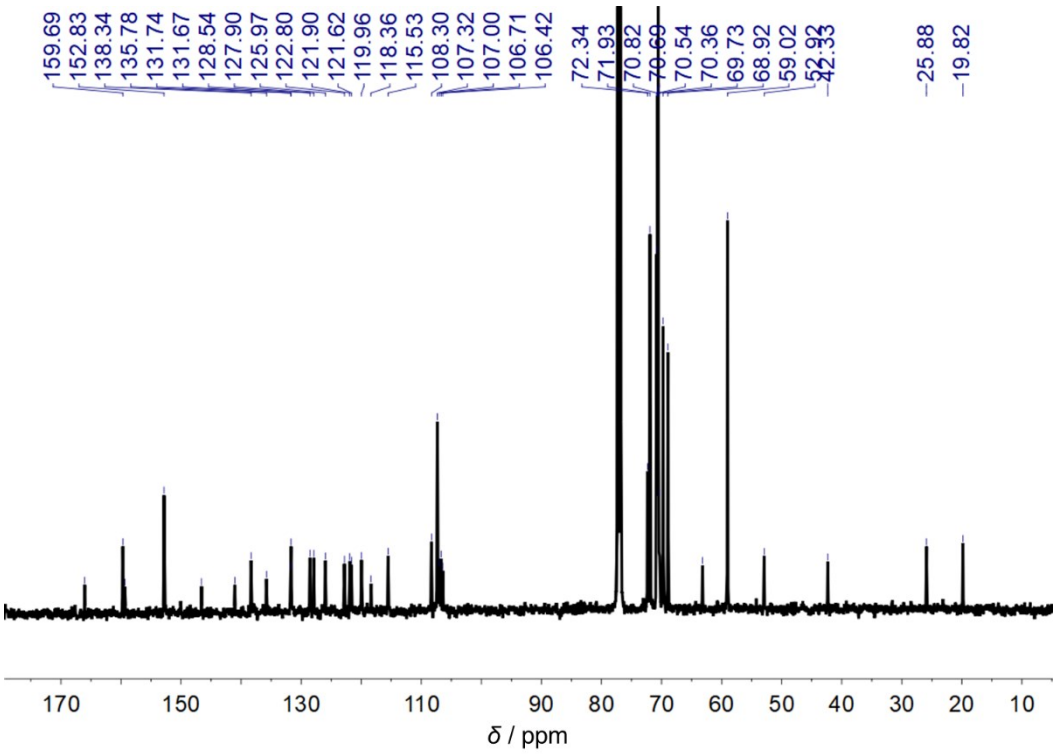

Figure S50. $^{13}C\{^{1}H\}$ NMR spectrum of compound **3** in $CDCl_3$ at room temperature.

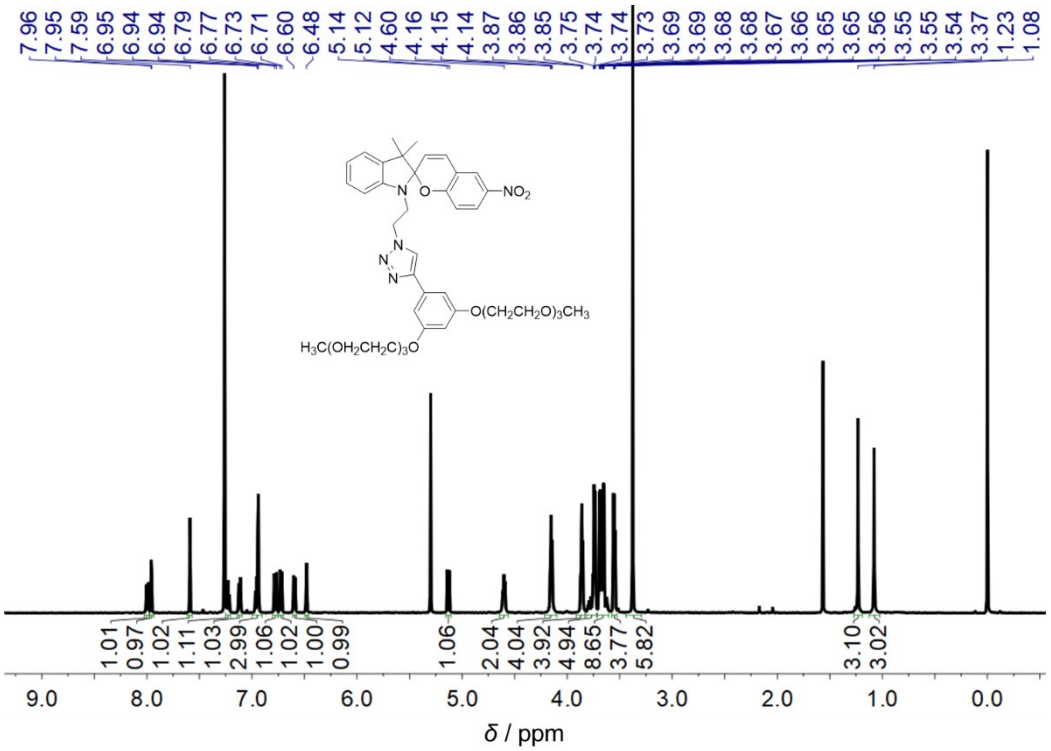

Figure S51. ^{1}H NMR spectrum of compound **4** in $CDCl_3$ at room temperature.

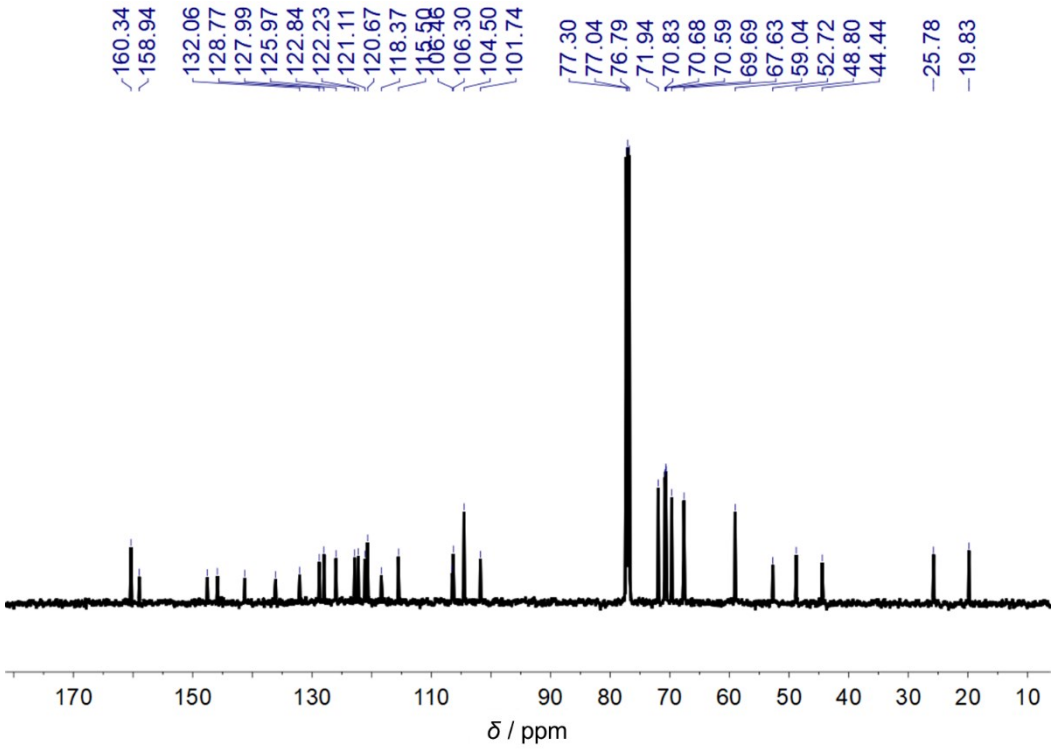

Figure S52. $^{13}C\{^{1}H\}$ NMR spectrum of compound **4** in $CDCl_3$ at room temperature.

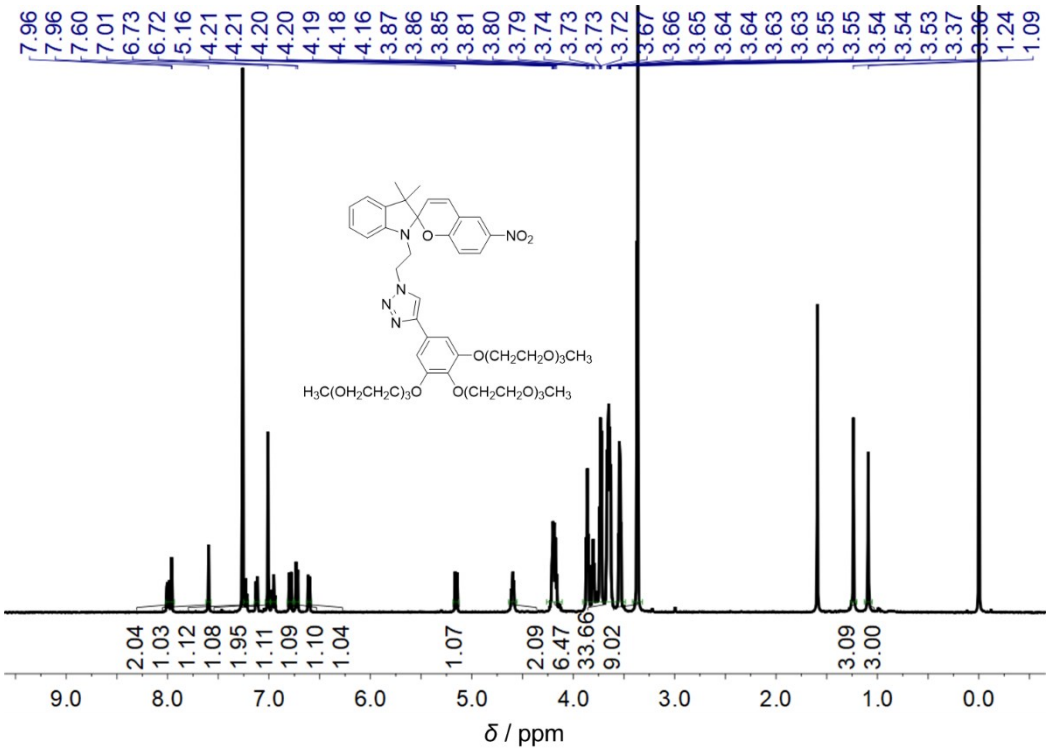

Figure S53. ^{1}H NMR spectrum of compound **5** in $CDCl_3$ at room temperature.

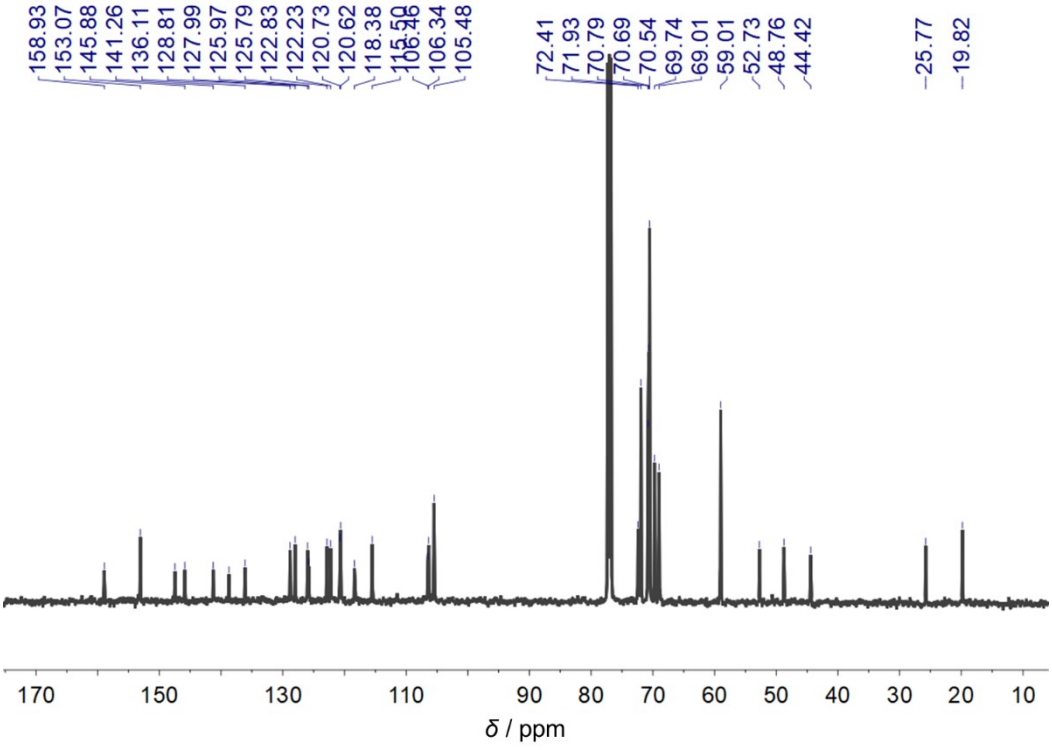

Figure S54. $^{13}C\{^{1}H\}$ NMR spectrum of compound **5** in $CDCl_3$ at room temperature.

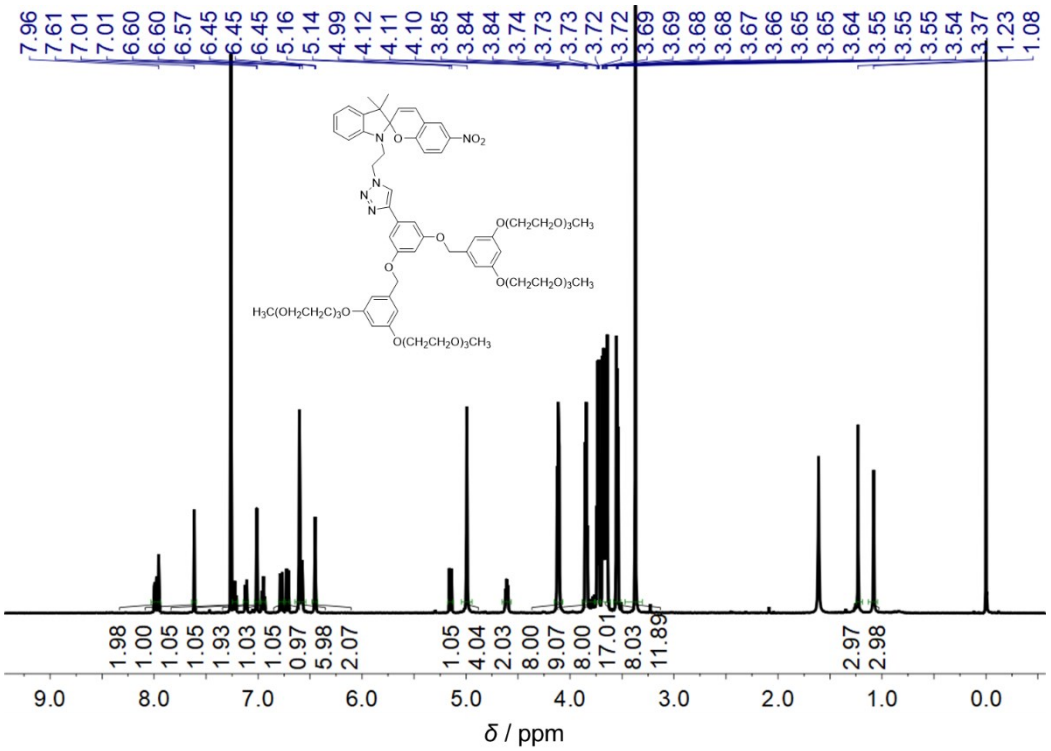

Figure S55. ^{1}H NMR spectrum of compound **6** in $CDCl_3$ at room temperature.

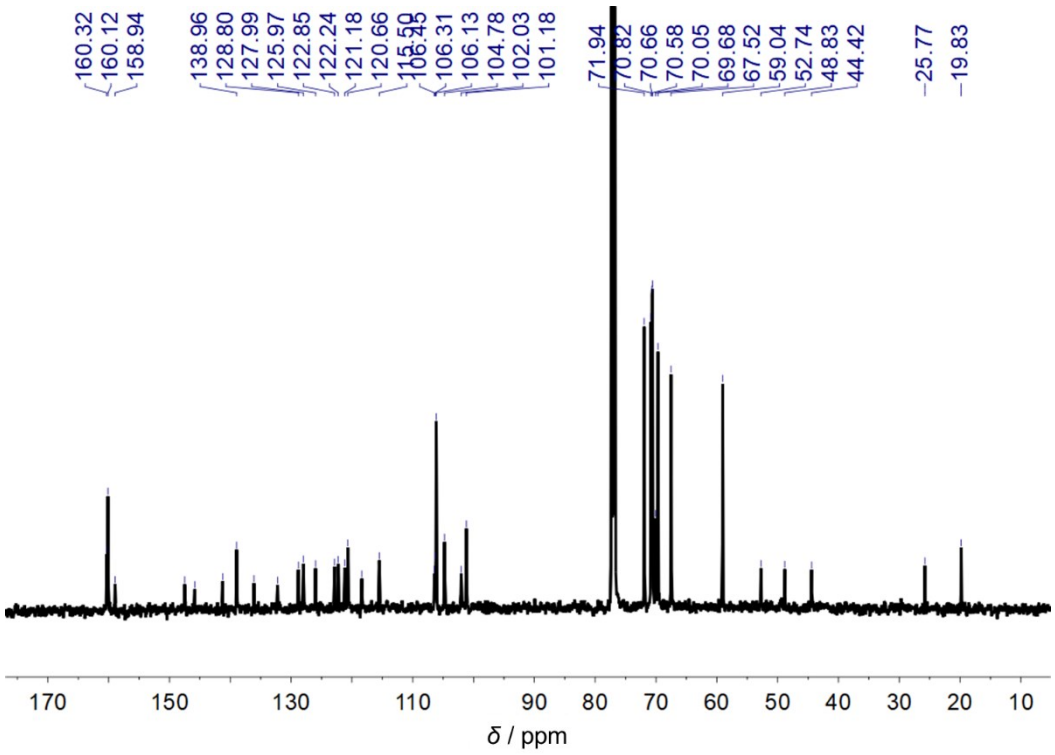

Figure S56. $^{13}C\{^{1}H\}$ NMR spectrum of compound **6** in $CDCl_3$ at room temperature.

Experimental section

Materials and reagents: 3,4,5-Trimethoxybenzoic acid, 1-bromo-3,4,5-trimethoxybenzene, 4-dimethylaminopyridine (DMAP), *N*,*N*'-dicyclohexylcarbodiimide (DCC), trimethylsilylacetylene (TMSA), copper(I) iodide (CuI), and potassium tetrachloroplatinate(II) ($K_2[PtCl_4]$) were purchased from Energy Chemical Co, Ltd. Sodium azide (NaN_3), copper(II) sulfate pentahydrate ($CuSO_4•5H_2O$), *N*,*N*-dimethylformamide (DMF), dichloromethane (DCM), diisopropanolamine (DIPA), tetrahydrofuran (THF), potassium carbonate (K_2CO_3) and sodium sulphate (Na_2SO_4) were products of Beijing Chemical Reagent Company. All commercially available reagents were of analytical grade and were used as received. All solvents were purified and distilled using standard procedures before use. Tetrakis(triphenylphosphine)palladium(0)[1] as catalysts for Sonogashira coupling reactions, 2-(3',3'-dimethyl-6-nitrospiro[chromene-2,2'-indolin]-1'-yl)ethan-1-ol (SP-OH),[2] 2-(3',3'-dimethyl-6-nitrospiro[chromene-2,2'-indolin]-1'-yl)ethyl 4-methylbenzenesulfonate (SP-OTs),[3] 1'-(2-azidoethyl)-3',3'-dimethyl-6-nitrospiro[chromene-2,2'-indoline] (SP-N_3),[4] 3,5-bis(triethyleneglycol methyl ether)benzoic acid (2TEG-Ph-COOH),[5] 3,4,5-tris(triethyleneglycol methyl ether)benzoic acid (3TEG-Ph-COOH),[5] 1-ethynyl-3,5-bis(triethyleneglycol methyl ether)benzene (2TEG-Ph-alkyne),[6] 5-ethynyl-1,2,3-tris(triethyleneglycol methyl ether)benzene (3TEG-Ph-alkyne),[7] 3,5-bis((3,4,5-tris(triethyleneglycol methyl ether)benzyl)oxy)benzoic acid (G2-3TEG-Ph-COOH),[8] and 5,5'-(((5-bromo-1,3-phenylene)bis(oxy))bis(methylene))bis(1,3-bis(triethyleneglycol methyl ether)benzene) (G2-2TEG-Ph-Br)[9] were synthesized according to the literature with slight modifications.

Synthesis and characterization

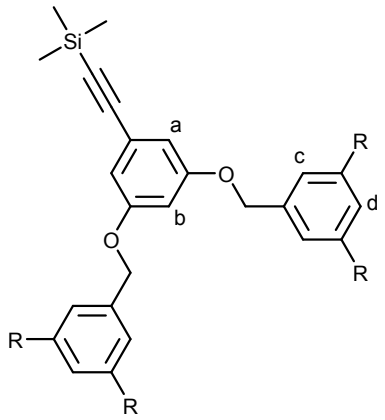

R = $O(CH_2CH_2O)_3CH_3$

L1 (G2-2TEG-Ph-TMSA). This was prepared through a Sonogashira coupling which has been described in the literature with slight modifications.[10] To a degassed diisopropanolamine solution (120 mL) of G2-2TEG-Ph-Br (4.00 g, 3.93 mmol) and trimethylsilylacetylene (TMSA) (1.50 g, 15.72 mmol) were added a catalytic amount of tetrakis(triphenylphosphine)palladium(0) (227.15 mg, 0.20 mmol) and CuI (37.50 mg, 0.20 mmol). The reaction mixture was heated to refluxed overnight under nitrogen. The resulting mixture was filtered and evaporated to dryness under reduced pressure. The crude product was purified by column chromatography on silica gel (100–200 mesh) using ethyl acetate-methanol (10:1 v/v) as the eluent to afford the product as a colorless oil. Yield: 2.35 g, 2.27 mmol (58 %). ^{1}H NMR (500 MHz, $CDCl_3$, 298 K, relative to Me_4Si): δ/ppm = 6.69 (d, J = 2.3 Hz, 2H; H_a), 6.59–6.54 (m, 5H; H_b, H_c), 6.44 (s, 2H; H_d), 4.93 (s, 4H; –OCH_2–), 4.14–4.06 (m, 8H; –OCH_2–), 3.87–3.81 (m, 8H; –CH_2O–), 3.76–3.71 (m, 8H; –OCH_2–), 3.70–3.63 (m, 16H; –CH_2–), 3.57–3.52 (m, 8H; –CH_2O–), 3.37 (s, 12H; –OCH_3), 0.25 (s, 9H; –$Si(CH_3)_3$).

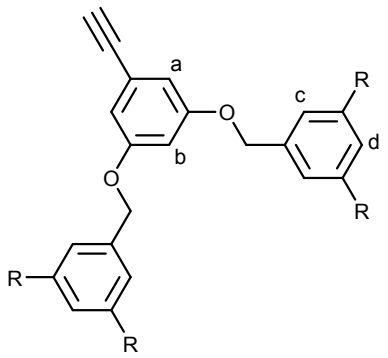

R = $O(CH_2CH_2O)_3CH_3$

L2 (G2-2TEG-Ph-alkyne). To a tetrahydrofuran solution (50 mL) of G2-2TEG-Ph-TMSA (2.35 g, 2.27 mmol) was added K_2CO_3 (1.16 g 9.08 mmol). The mixture was stirred overnight at room temperature, then deionized water was added. The organic part was extracted with chloroform, dried over anhydrous Na_2SO_4 and evaporated to dryness under reduced pressure. The crude product was purified by column chromatography on silica gel (100–200 mesh) using ethyl acetate-methanol (10:1 v/v) as the eluent to afford the product as a colorless oil. Yield: 2.05 g, 2.13 mmol (94 %). ^{1}H NMR (500 MHz, $CDCl_3$, 298 K, relative to Me_4Si): δ/ppm = 6.70 (d, J = 2.1 Hz, 2H; H_a), 6.60–6.58 (m, 1H; H_b), 6.57 (d, J = 1.8 Hz, 4H; H_c), 6.44 (s, 2H; H_d), 4.93 (s, 4H; –OCH_2–), 4.13–4.08 (m, 8H; –OCH_2–), 3.87–3.82 (m, 8H; –CH_2O–), 3.76–3.70 (m, 8H; –OCH_2–), 3.69–3.62 (m, 16H; –CH_2–), 3.57–3.52 (m, 8H; –CH_2O–), 3.37 (s, 12H; –OCH_3), 3.03 (s, 1H; –C≡CH).

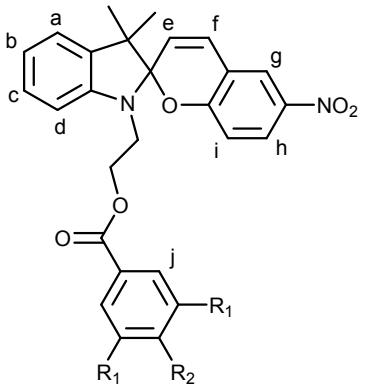

1 $R_1 = O(CH_2CH_2O)_3CH_3$ $R_2 = H$

2 $R_1 = R_2 = O(CH_2CH_2O)_3CH_3$

Compound **1**. To a degassed solution of SP-OH (960 mg, 2.75 mmol), 2TEG-Ph-COOH (1.47 g, 3.30 mmol) and catalytic amount of 4-dimethylaminopyridine (DMAP) (37.5 mg, 0.31 mmol) in dry dichloromethane (60 mL) was added *N*,*N*'-dicyclohexylcarbodiimide (DCC) (684 mg, 3.32 mmol). The resulting solution was allowed to stir at room temperature for 36 h under nitrogen atmosphere. After filtering off the resulting *N*,*N*'-dicyclohexylurea (DCU), the solvent was removed under reduced pressure to obtain the residue, which was purified by column chromatography on silica gel (100–200 mesh) in the dark using ethyl acetate as the eluent to afford the product as an oil with a pale blue tint. Yield: 1.21 g, 1.55 mmol (56 %). ^{1}H NMR (500 MHz, $CDCl_3$, 298 K, relative to Me_4Si): δ/ppm = 8.00–7.95 (m, 2H; H_h, H_g), 7.24–7.18 (m, 1H; H_c), 7.12–7.06 (m, 3H; H_j, H_a), 6.93–6.86 (m, 2H; H_b, R_2), 6.77–6.70 (m, 2H; H_f, H_i), 6.69–6.64 (m, 1H; H_d), 5.86 (d, J = 10.3 Hz, 1H; H_e), 4.48–4.39 (m, 2H; –CH_2O–), 4.12–4.05 (m, 4H; –OCH_2–), 3.89–3.81 (m, 4H; –CH_2O–), 3.77–3.71 (m, 4H; –OCH_2–), 3.71–3.63 (m, 10H; –CH_2OCH_2–, –NCH_2–), 3.58–3.52 (m, 4H; –CH_2O–), 3.37 (s, 6H; –OCH_3), 1.28 (s, 3H; –CH_3), 1.16 (s, 3H; –CH_3). ^{13}C{^{1}H} NMR (125 MHz, $CDCl_3$, 298 K): δ/ppm = 166.08, 159.78, 159.36, 146.66, 141.08, 135.76, 131.57, 128.46, 127.92, 125.98, 122.83, 121.87, 121.67, 119.95, 118.39, 115.53, 108.03, 106.89, 106.71, 106.44, 71.95, 70.86, 70.68, 70.60, 69.58, 67.75, 63.07, 59.05, 52.86, 42.42, 25.90, 19.83. Positive HR-ESI MS: calcd for $[C_{41}H_{53}N_2O_{13}]^+$ m/z 781.3548; found 781.3542 $[M+H]^+$. Elemental analysis calcd (%) for $C_{41}H_{52}N_2O_{13}$: C 63.06, H 6.71, N 3.59; found: C 63.04, H 6.76, N 3.42.

Compound **2**. This was prepared from a similar procedure as that of compound **1**, except 3TEG-Ph-COOH (1.13 g, 1.86 mmol) was used instead of 2TEG-Ph-COOH. Yield: 724.32 mg, 0.9 mmol (58 %). ^{1}H NMR (500 MHz, $CDCl_3$, 298 K, relative to Me_4Si): δ/ppm = 8.04–7.96 (m, 2H; H_h, H_g), 7.25–7.17 (m, 3H; H_j, H_c), 7.09 (d, J = 6.8 Hz, 1H; H_a), 6.93–6.86 (m, 2H; H_b, H_f), 6.80–6.71 (m, 2H; H_i, H_d), 5.87 (d, J = 10.3 Hz, 1H; H_e), 4.42 (t, J = 6.3 Hz, 2H; –CH_2O–), 4.25–4.18 (m, 2H; –OCH_2–), 4.17–4.07 (m, 4H; –OCH_2–), 3.90–3.47 (m, 32H; –CH_2–, –NCH_2–), 3.37 (s, 9H; –OCH_3), 1.28 (s, 3H; –CH_3), 1.16 (s, 3H; –CH_3). ^{13}C{^{1}H} NMR (125 MHz, $CDCl_3$, 298 K): δ/ppm = 165.94, 159.36, 152.32, 146.77, 142.75, 141.12, 135.74, 128.45, 127.92, 126.00, 124.59, 122.83, 121.86, 121.66, 119.95, 118.40, 115.57, 108.95, 106.74,

106.48, 72.45, 71.94, 70.84, 70.70, 70.58, 69.59, 68.84, 63.00, 59.03, 52.83, 42.41, 25.92, 19.83. Positive HR-ESI MS: calcd for $[C_{48}H_{67}N_2O_{17}]^+$ *m*/*z* 943.4440; found 943.4434 $[M+H]^+$. Elemental analysis calcd (%) for $C_{48}H_{66}N_2O_{17}$: C 61.13, H 7.05, N 2.97; found: C 61.14, H 7.08, N 2.85.

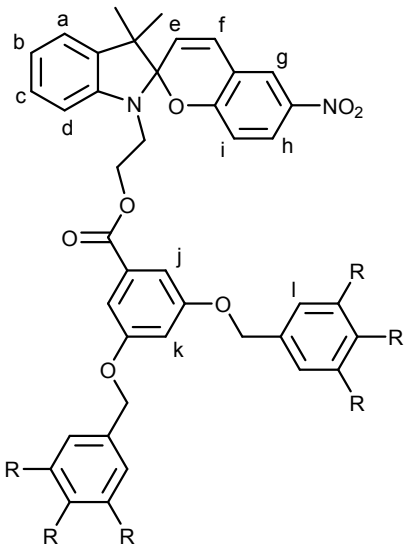

3 R = $O(CH_2CH_2O)_3CH_3$

Compound **3**. This was prepared from a similar procedure as that of compound **1**, except G2-3TEG-Ph-COOH (727 mg, 0.56 mmol) was used instead of 2TEG-Ph-COOH. Yield: 427 mg, 0.26 mmol (56 %). ^{1}H NMR (500 MHz, $CDCl_3$, 298 K, relative to Me_4Si): δ/ppm = 7.97–7.91 (m, 2H; H_h, H_g), 7.23–7.14 (m, 3H; H_c, H_j), 7.09 (d, J = 7.3 Hz, 1H; H_a), 6.92–6.85 (m, 2H; H_b, H_f), 6.79–6.60 (m, 7H; H_k, H_i, H_d, H_l), 5.86 (d, J = 10.4 Hz, 1H; H_e), 4.89 (s, 4H; –OCH_2–), 4.52–4.39 (m, 2H; –CH_2O–), 4.25–4.10 (m, 12H; –OCH_2–), 3.90–3.47 (m, 62H; CH_2, –NCH_2–), 3.41–3.29 (m, 18H; –OCH_3), 1.26 (s, 3H; –CH_3), 1.16 (s, 3H; –CH_3). $^{13}C\{^1H\}$ NMR (125 MHz, $CDCl_3$, 298 K): δ/ppm = 166.03, 159.69, 159.35, 152.83, 146.59, 141.05, 138.34, 135.78, 131.74, 131.67, 128.54, 127.90, 125.97, 122.80, 121.90, 121.62, 119.96, 118.36, 115.53, 108.30, 107.32, 107.00, 106.71, 106.42, 72.34, 71.93, 70.82, 70.69, 70.54, 70.36, 69.73, 68.92, 63.18, 59.02, 52.92, 42.33, 25.88, 19.82. Positive HR-ESI MS: calcd for $[C_{83}H_{121}N_2O_{31}]^+$ *m*/*z* 1641.7953; found 1641.7949 $[M+H]^+$. Elemental analysis calcd (%) for $C_{83}H_{120}N_2O_{31}$: C 60.72, H 7.37, N 1.71; found: C 60.86, H 7.32, N 1.59.

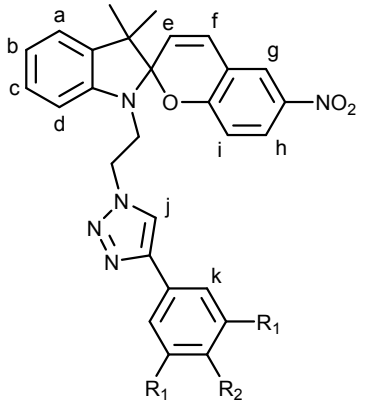

4 $R_1 = O(CH_2CH_2O)_3CH_3$ $R_2 = H$

5 $R_1 = R_2 = O(CH_2CH_2O)_3CH_3$

Compound **4**. This was prepared according to a modification of the procedures for azide-alkyne click reaction in the literature.[4,11] To a solution of SP-N_3 (315 mg, 0.83mmol) and 2TEG-Ph-alkyne (295 mg, 0.69 mmol) in dichloromethane (30 mL) were added sodium ascorbate (100 mg, 0.50 mmol) and $CuSO_4$•$5H_2O$ (253 mg, 1.01 mmol) in deionized water (20 mL). The mixture was stirred at room temperature under nitrogen atmosphere overnight. The organic phase was separated and washed by deionized water, and was dried over anhydrous Na_2SO_4. After the solvent was removed under reduced pressure, the crude product was purified by column chromatography on silica gel (100–200 mesh) in the dark with ethyl acetate-methanol (10:1 v/v) as the eluent to give the product as an oil with a pale blue tint. Yield: 556 mg, 0.59 mmol (86 %). ^{1}H NMR (500 MHz, $CDCl_3$, 298 K, relative to Me_4Si): δ/ppm = 8.05–7.96 (m, 2H; H_h, H_g), 7.61 (s, 1H; H_j), 7.25 (t, J = 7.3 Hz, 1H; H_c), 7.14 (d, J = 7.3 Hz, 1H; H_a), 7.02–6.92 (m, 3H; H_b, H_k), 6.80 (d, J = 10.4 Hz, 1H; H_f), 6.75 (d, J = 8.9 Hz, 1H; H_i), 6.62 (d, J = 7.3 Hz, 1H; H_d), 6.51 (s, 1H; R_2), 5.16 (d, J = 10.4 Hz, 1H; H_e), 4.67–4.58 (m, 2H; –CH_2N–), 4.24–4.12 (m, 4H; –OCH_2–), 3.94–3.53 (m, 22H; CH_2, –NCH_2–), 3.40 (s, 6H; –OCH_3), 1.27 (s, 3H; –CH_3), 1.10 (s, 3H; –CH_3). ^{13}C{^{1}H} NMR (125 MHz, $CDCl_3$, 298 K): δ/ppm = 160.34, 158.94, 147.56, 145.85, 141.26, 136.10, 132.06, 128.77, 127.99, 125.97, 122.84, 122.23, 121.11, 120.67, 118.37, 115.50, 106.46, 106.30, 104.50, 101.74, 71.94, 70.83, 70.68, 70.59, 69.69, 67.63, 59.04, 52.72, 48.80, 44.44, 25.78, 19.83. Positive HR-ESI MS: calcd for $[C_{42}H_{54}N_5O_{11}]^+$ m/z 804.3820; found 804.3814 $[M+H]^+$. Elemental analysis calcd (%) for $C_{42}H_{53}N_5O_{11}$: C 62.75, H 6.65, N 8.71; found: C 62.37, H 6.64, N 8.45.

Compound **5**. This was prepared from a similar procedure as that of compound **4**, except 3TEG-Ph-alkyne (490 mg, 0.83 mmol) was used instead of 2TEG-Ph-alkyne. Yield: 773 mg, 0.67 mmol (81 %). ^{1}H NMR (500 MHz, $CDCl_3$, 298 K, relative to Me_4Si): δ/ppm = 8.03–7.94 (m, 2H; H_h, H_g), 7.60 (s, 1H; H_j), 7.23 (t, J = 7.3 Hz, 1H; H_c), 7.12 (d, J = 7.3 Hz, 1H; H_a), 7.01 (s, 2H; H_k), 6.95 (t, J = 7.3 Hz, 1H; H_b), 6.79 (d, J = 10.4 Hz, 1H; H_f), 6.73 (d, J = 8.8 Hz, 1H; H_i), 6.61 (d, J = 7.3 Hz, 1H; H_d), 5.15 (d, J = 10.4 Hz, 1H; H_e), 4.64–4.55 (m, 2H; –CH_2N–), 4.26–4.11 (m, 6H; –OCH_2–), 3.91–3.47 (m, 32H; CH_2, –NCH_2–), 3.42–3.32 (m, 9H; –OCH_3), 1.24 (s, 3H; –CCH_3), 1.09 (s, 3H; –CCH_3). ^{13}C{^{1}H} NMR (125 MHz, $CDCl_3$, 298 K): δ/ppm = 158.93, 153.07, 147.47, 145.88, 141.26, 138.72, 136.11, 128.81, 127.99, 125.97, 125.79, 122.83, 122.23, 120.73, 120.62, 118.38, 115.50, 106.46, 106.34, 105.48, 72.41, 71.93, 70.79, 70.69, 70.54, 69.74, 69.01, 59.01, 52.73, 48.76, 44.42, 25.77, 19.82. Positive HR-ESI MS: calcd for $[C_{49}H_{68}N_5O_{15}]^+$ m/z 966.4712; found 966.4706 $[M+H]^+$. Elemental analysis calcd (%) for $C_{49}H_{67}N_5O_{15}$: C 60.92, H 6.99, N 7.25; found: C 60.54, H 7.09, N 6.88.

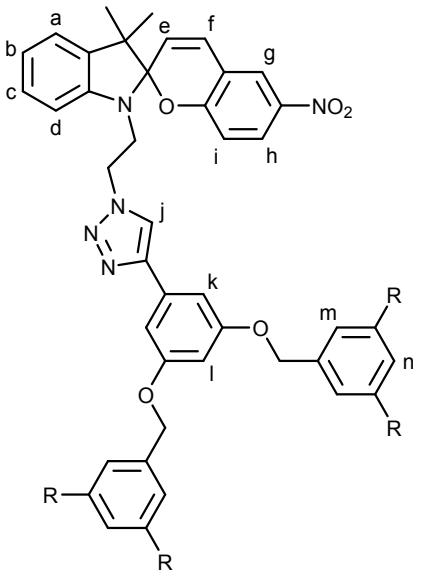

6 R = $O(CH_2CH_2O)_3CH_3$

Compound **6**. This was prepared from a similar procedure as that of compound **4**, except G2-2TEG-Ph-alkyne (490 mg, 0.51 mmol) was used instead of 2TEG-Ph-alkyne. Yield: 576 mg, 0.43 mmol (84%). ^{1}H NMR (500 MHz, $CDCl_3$, 298 K, relative to Me_4Si): δ/ppm = 8.03–7.94 (m, 2H; H_h, H_g), 7.61 (s, 1H; H_j), 7.22 (d, J = 7.3 Hz, 1H; H_c), 7.12 (d, J = 7.3 Hz, 1H; H_a), 7.01

(s, 2H; H_k), 6.95 (t, J = 7.3 Hz, 1H; H_b), 6.78 (d, J = 10.4 Hz, 1H; H_f), 6.72 (d, J = 8.9 Hz, 1H; H_i), 6.65–6.54 (m, 6H; H_m, H_d, H_l), 6.45 (s, 2H; H_n), 5.15 (d, J = 10.4 Hz, 1H; H_e), 4.99 (s, 4H; $-OCH_2-$), 4.65–4.57 (m, 2H; $-CH_2O-$), 4.15–4.07 (m, 8H; $-OCH_2-$), 3.88–3.76 (m, 8H; $-CH_2O-$), 3.76–3.61 (m, 26H; $-CH_2-$, $-NCH_2-$), 3.58–3.51 (m, 8H; $-CH_2O-$), 3.37 (s, 12H; $-OCH_3$), 1.23 (s, 3H; $-CH_3$), 1.08 (s, 3H; $-CH_3$). $^{13}C\{^1H\}$ NMR (125 MHz, $CDCl_3$, 298 K): δ/ppm = 160.32, 160.12, 158.94, 147.49, 145.85, 141.26, 138.96, 136.11, 132.22, 128.80, 127.99, 125.97, 122.85, 122.24, 121.18, 120.66, 118.38, 115.50, 106.45, 106.31, 106.13, 104.78, 102.03, 101.18, 71.94, 70.82, 70.66, 70.58, 70.05, 69.68, 67.52, 59.04, 52.74, 48.83, 44.42, 25.77, 19.83. Positive HR-ESI MS: calcd for $[C_{70}H_{94}N_5O_{21}]^+$ m/z 1340.6441; found 1340.6436 $[M+H]^+$. Elemental analysis calcd (%) for $C_{70}H_{93}N_5O_{21}$: C 62.72, H 6.99, N 5.22; found: C 62.39, H 6.96, N 5.00.

Physical measurements and instrumentation

^1H NMR (500 MHz) and $^{13}C\{^1H\}$ NMR (125 MHz) spectra were obtained on a Bruker DRX 500 (500 MHz) spectrometer at 298 K with chemical shifts reported relative to tetramethylsilane (Me_4Si). Positive-ion electrospray ionization (ESI) mass spectra were recorded on a Bruker maXis II ESI-QTOF mass spectrometer. Elemental analysis was carried out on a Flash EA1112 analyzer from ThermoQuest Italia S.P.A. UV-Vis absorption spectra were recorded using a Varian Cary 50 UV-vis spectrophotometer. Steady-state excitation and emission spectra at room temperature were obtained on an Edinburgh Instruments FS5 spectrofluorometer. Photoirradiation was carried out using a 300 W Oriel Corporation Model 60011 Xe (ozone-free) lamp, and monochromatic light was obtained by passing the light through an Applied Photophysics F 3.4 monochromator, and the path length of optical cuvettes is 1 cm. Dynamic light scattering (DLS) measurements were performed by using a Malvern Zetasizer NanoZS instrument. Transmission electron microscopic (TEM) images were obtained with a JEM-2100F electron microscope operating at 200 kV. Atomic force microscope (AFM) measurements were carried out on a Bruker FastScan atomic force microscope. Fluorescence

microscopy images were obtained from fluorescence microscopy (Vision Engineering Co., UK).

The thermal bleaching reaction of spiropyran is known to follow first order kinetics at various temperatures. The kinetics for the bleaching reaction were determined by measurement of the UV-vis spectral changes at various temperatures by use of a Varian Cary 50 UV-vis spectrophotometer, with the temperature controlled by a Varian Cary single cell Peltier thermostat. The first-order rate constants were obtained by taking the negative value of the slope of a linear least-squares fit of ln $[(A - A_\infty)/(A_0 - A_\infty)]$ against time according to Equation(1),

$$\ln [(A - A_\infty)/(A_0 - A_\infty)] = - kt \quad (1)$$

where A, A_0, and A_∞ are the absorbances at the absorption wavelength maximum of the photomerocyanine at times t, 0 and infinity, respectively and k is the rate constant of the reaction. The kinetics parameters were obtained by a linear least-squares fitting of ln (k/T) against $1/T$ according to the linear expression of the Eying equation (2), ln k against $1/T$ according to the Arrhenius equation (3), and the change in Gibbs free energy of activation ($\Delta G^{\neq}$) at 298 K were determined according to equation (4),

$$\ln (k/T) = - (\Delta H^{\neq}/R) (1/T) + \ln (k_B h^{-1}) + (\Delta S^{\neq}/R) \quad (2)$$

$$\ln (k) = - E_a/RT + \ln A \quad (3)$$

$$\Delta G^{\neq} = \Delta H^{\neq} - T \Delta S^{\neq} \quad (4)$$

where $\Delta H^{\neq}$ and $\Delta S^{\neq}$ are the changes in activation enthalpy and entropy, respectively, T is the temperature, and k_B, R, h, and A are the Boltzmann's constant, the universal gas constant, the Planck constant and the frequency factor, respectively.

Sample preparation

The samples for TEM measurements were prepared by adding a few drops of solutions onto a carbon-coated copper grid. They were then dried in air until the solvent was completely evaporated off in the dark. The sample preparation for AFM measurements was the same as that for TEM except that 10 μL of solution was dropped onto a silicon wafer. The sample solutions for DLS measurements were filtered and allowed to stand under room conditions for 2 min before tests.

Computational details

All calculations in this study were performed with the Gaussian 09 suite of programs.[12] By density functional theory (DFT), the ground-state (S_0) geometries of the closed and open forms of compound **5** were fully optimized in THF solution with the long range corrected B3LYP functional using the Coulomb-attenuating method (CAM-B3LYP),[13] in conjunction with the polarizable continuum model (PCM).[14] On the basis of the optimized S_0 geometries of the open and closed forms of **5**, time-dependent DFT (TDDFT)[15–17] calculations were performed for the computation of the singlet–singlet transitions in the electronic absorption spectra. In order to investigate the noncovalent interactions in the dimeric form of **5**, the geometry of the dimer of the open merocyanine form of **5** was optimized with the PBE0-D3(BJ) functional[18–22] in THF–*n*-hexane (1 : 9 v/v) solution, and noncovalent interactions (NCI) analysis was performed on the optimized geometry with NCIPLOT.[23] The Cartesian coordinates of the optimized S_0 geometries of the closed and open forms of compound **5**, as well as the dimer of the open form, are given in Table S2–S4 respectively. Vibrational frequencies of all the optimized geometries have been computed and all of them were confirmed to be minima on the potential energy surface, as there are no imaginary frequencies observed (NIMAG = 0). For all the calculations, the 6-31G(d,p) basis set[24–27] was employed to describe all the atoms, and a pruned (99,590) grid was employed for numerical integration.

Isokinetic relationship

When a series of structurally related substrates undergo the same general reaction or when the reaction conditions for a single substrate are changed in a systematic way, the enthalpies and entropies of activation sometimes satisfy the relation,[28]

$$\Delta H^{\neq} - \beta \Delta S^{\neq} = \text{constant}$$

where the parameter β is independent of temperature. This equation represents an 'isokinetic relationship'. The temperature $T = \beta$, at which all members of a series obeying the isokinetic relationship react at the same rate, is termed the 'isokinetic temperature'.

References

1. D. R. Coulson, L. C. Satek and S. O. Grim, Tetrakis (triphenylphosphine) palladium(0), *Inorg. Synth.*, 1972, **13**, 121−124.
2. F. M. Raymo and S. Giordani, Signal processing at the molecular level, *J. Am. Chem. Soc.*, 2001, **123**, 4651−4652.
3. J. Yan, L. X. Zhao, C. Li, Z. Hu, G. F. Zhang, Z. Q. Chen, T. Chen, Z. L. Huang, J. Zhu and M. Q. Zhu, Optical nanoimaging for block copolymer self-assembly, *J. Am. Chem. Soc.* 2015, **137**, 2436−2439.
4. Y. Zhang, M. Ng, E. Y.-H. Hong, A. K.-W. Chan, N. M.-W. Wu, M. H.-Y. Chan, L. Wu and V. W.-W. Yam, Synthesis and photoswitchable amphiphilicity and self-assembly properties of photochromic spiropyran derivatives, *J. Mater. Chem. C*, 2020, **8**, 13676−13685.
5. S. Zhang, H.-J. Sun, A. D. Hughes, B. Draghici, J. Lejnieks, P. Leowanawat, A. Bertin, L. Otero De Leon, O. V. Kulikov, Y. Chen, D. J. Pochan, P. A. Heiney and V. Percec, "Single-single" amphiphilic janus dendrimers self-assemble into uniform dendrimersomes with predictable size, *ACS Nano*, 2014, **8**, 1554−1565.
6. C. Po and V. W-W. Yam, A metallo-amphiphile with unusual memory behaviour: effect of temperature and structure on the self-assembly of triethylene glycol (TEG)-pendant platinum(II) bzimpy complexes, *Chem. Sci.*, 2014, **5**, 4868−4872.
7. X. Li, C.-T. Poon, E. Y.-H. Hong, H.-L. Wong, A. K.-W. Chan, L. Wu and V. W-W. Yam, Multi-modulation for self-assemblies of amphiphilic rigid-soft compounds through alteration of solution polarity and temperature, *Soft Matter*, 2017, **13**, 8408−8418.
8. K. C. Elbert, D. Jishkariani, Y. Wu, J. D. Lee, B. Donnio and C. B. Murray, Design, self-assembly, and switchable wettability in hydrophobic, hydrophilic, and janus dendritic ligand-gold nanoparticle hybrid materials, *Chem. Mater.*, 2017, **29**, 8737−8746.
9. H. Chen, Y. Yang, Y. Wang and L. Wu, Synthesis, structural characterization, and thermoresponsivity of hybrid supramolecular dendrimers bearing a polyoxometalate core, *Chem. - Eur. J.*, 2013, **19**, 11051−11061.
10. M. H.-Y. Chan, S. Y.-L. Leung and V. W-W. Yam, Rational design of multi-stimuli-responsive scaffolds: synthesis of luminescent oligo(ethynylpyridine)-containing alkynylplatinum(II) polypyridine foldamers stabilized by Pt···Pt interactions, *J. Am. Chem. Soc.*, 2019, **141**, 1231−12321.
11. L. Kong, H.-L. Wong, A. Y.-Y. Tam, W. H. Lam, L. Wu and V. W.-W. Yam, Synthesis, characterization, and photophysical properties of bodipy-spirooxazine and -spiropyran conjugates: modulation of fluorescence resonance energy transfer behavior via acidochromic and photochromic switching, *ACS Appl. Mater. Interfaces*, 2014, **6**, 1550−1562.
12. M. J. Frisch, G. W. Trucks, H. B. Schlegel, G. E. Scuseria, M. A. Robb, J. R. Cheeseman, G. Scalmani, V. Barone, B. Mennucci, G. A. Petersson, H. Nakatsuji, M. Caricato, X. Li, H. P. Hratchian, A. F. Izmaylov, J. Bloino, G. Zheng, J. L. Sonnenberg, M. Hada, M. Ehara, K. Toyota, R. Fukuda, J. Hasegawa, M. Ishida, T. Nakajima, Y.

Honda, O. Kitao, H. Nakai, T. Vreven, Jr. Montgomery, J. A., J. E. Peralta, F. Ogliaro, M. Bearpark, J. J. Heyd, E. Brothers, K. N. Kudin, V. N. Staroverov, T. Keith, R. Kobayashi, J. Normand, K. Raghavachari, A. Rendell, J. C. Burant, S. S. Iyengar, J. Tomasi, M. Cossi, N. Rega, J. M. Millam, M. Klene, J. E. Knox, J. B. Cross, V. Bakken, C. Adamo, J. Jaramillo, R. Gomperts, R. E. Stratmann, O. Yazyev, A. J. Austin, R. Cammi, C. Pomelli, J. W. Ochterski, R. L. Martin, K. Morokuma, V. G. Zakrzewski, G. A. Voth, P. Salvador, J. J. Dannenberg, S. Dapprich, A. D. Daniels, O. Farkas, J. B. Foresman, J. V. Ortiz, J. Cioslowski and D. J. Fox, Gaussian 09 (Revision D.01), Gaussian, Inc.: Wallingford CT, 2013.

13. T. Yanai, D. P. Tew and N. C. Handy, A new hybrid exchange-correlation functional using the coulomb-attenuating method (CAM-B3LYP), *Chem. Phys. Lett.*, 2004, **393**, 51–57.
14. M. Cossi, G. Scalmani, N. Rega and V. Barone, New developments in the polarizable continuum model for quantum mechanical and classical calculations on molecules in solution, *J. Chem. Phys*., 2002, **117**, 43–54.
15. R. E. Stratmann, G. E. Scuseria and M. J. Frisch, An efficient implementation of time-dependent density-functional theory for the calculation of excitation energies of large molecules, *J. Chem. Phys.*, 1998, **109**, 8218–8224.
16. R. Bauernschmitt and R. Ahlrichs, Treatment of electronic excitations within the adiabatic approximation of time dependent density functional theory, *Chem. Phys. Lett.*, 1996, **256**, 454–464.
17. M. E. Casida, C. Jamorski, K. C. Casida and D. R. Salahub, Molecular excitation energies to high-lying bound states from time-dependent density-functional response theory: characterization and correction of the time-dependent local density approximation ionization threshold, *J. Chem. Phys.*, 1998, **108**, 4439–4449.
18. C. Adamo and V. Barone, Toward reliable density functional methods without adjustable parameters: the PBE0 mode, *J. Chem. Phys*., 1999, **110**, 6158–6170.
19. S. Grimme, J. Antony, S. Ehrlich and H. Krieg, A consistent and accurate ab initio parametrization of density functional dispersion correction (DFT-D) for the 94 elements H-Pu, *J. Chem. Phys.*, 2010, **132**, 154104.
20. A. D. Becke and E. R. Johnson, A density-functional model of the dispersion interaction, *J. Chem. Phys.*, 2005, **123**, 154101.
21. E. R. Johnson and A. D. Becke, A post-hartree-fock model of intermolecular interactions, *J. Chem. Phys*., 2005, **123**, 024101.
22. E. R. Johnson and A. D. Becke, A post-hartree-fock model of intermolecular interactions: inclusion of higher-order corrections, *J. Chem. Phys*., 2006, **124**, 174104.
23. J. Contreras-García, E. R. Johnson, S. Keinan, R. Chaudret, J.-P. Piquemal, D. N. Beratan and W. Yang, NCIPLOT: a program for plotting noncovalent interaction regions, *J. Chem. Theory Comput*., 2011, **7**, 625–632.
24. W. J. Hehre, R. Ditchfie and J. A. Pople, Self-consistent molecular orbital methods. XII. Further extensions of Gaussian-type basis sets for use in molecular orbital studies of organic molecules, *J. Chem. Phys.*, 1972, **56**, 2257–2261.
25. P. C. Hariharan and J. A. Pople, The influence of polarization functions on molecular

orbital hydrogenation energies, *Theor. Chim. Acta*, 1973, **28**, 213–222.

26. J. D. Dill and J. A. Pople, Self-consistent molecular orbital methods. XV. Extended Gaussian-type basis sets for lithium, beryllium, and boron, *J. Chem. Phys.*, 1975, **62**, 2921–2923.
27. M. M. Francl, W. J. Pietro, W. J. Hehre, J. S. Binkley, M. S. Gordon, D. J. Defrees and J. A. Pople, Self-consistent molecular orbital methods. XXIII. A polarization-type basis set for second-row elements, *J. Chem. Phys.*, 1982, **77**, 3654–3665.
28. P. Muller, Glossary of terms used in physical organic chemistry (IUPAC Recommendations 1994). *Pure & Appl. Chem.*, 1994; **66**, 1077–1184.